



# Global Phase Diagrams of Frustrated Quantum Antiferromagnets in Two Dimensions: Doubled Chern-Simons Theory

## Citation

Xu, Cenke, and Subir Sachdev. 2009. Global phase diagrams of frustrated quantum antiferromagnets in two dimensions: doubled Chern-Simons theory. *Physical Review B* 79(6): 064405.

## Published Version

doi:10.1103/PhysRevB.79.064405

## Permanent link

<http://nrs.harvard.edu/urn-3:HUL.InstRepos:7459594>

## Terms of Use

This article was downloaded from Harvard University's DASH repository, and is made available under the terms and conditions applicable to Open Access Policy Articles, as set forth at <http://nrs.harvard.edu/urn-3:HUL.InstRepos:dash.current.terms-of-use#OAP>

## Share Your Story

The Harvard community has made this article openly available.  
Please share how this access benefits you. [Submit a story](#).

[Accessibility](#)

# Global phase diagrams of frustrated quantum antiferromagnets in two dimensions: doubled Chern-Simons theory

Cenke Xu and Subir Sachdev

*Department of Physics, Harvard University, Cambridge MA 02138, USA*

(Dated: January 2, 2009)

## Abstract

We present a general approach to understanding the quantum phases and phase transitions of quantum antiferromagnets in two spatial dimensions. We begin with the simplest spin liquid state, the  $Z_2$  spin liquid, whose elementary excitations are spinons and visons, carrying  $Z_2$  electric and magnetic charges respectively. Their dynamics are expressed in terms of a doubled U(1) Chern Simons theory, which correctly captures the ‘topological’ order of the  $Z_2$  spin liquid state. We show that the same theory also yields a description of the variety of ordered phases obtained when one or more of the elementary excitations condense. Field theories for the transitions and multicritical points between these phases are obtained. We survey experimental results on antiferromagnets on the anisotropic triangular lattice, and make connections between their phase diagrams and our results.

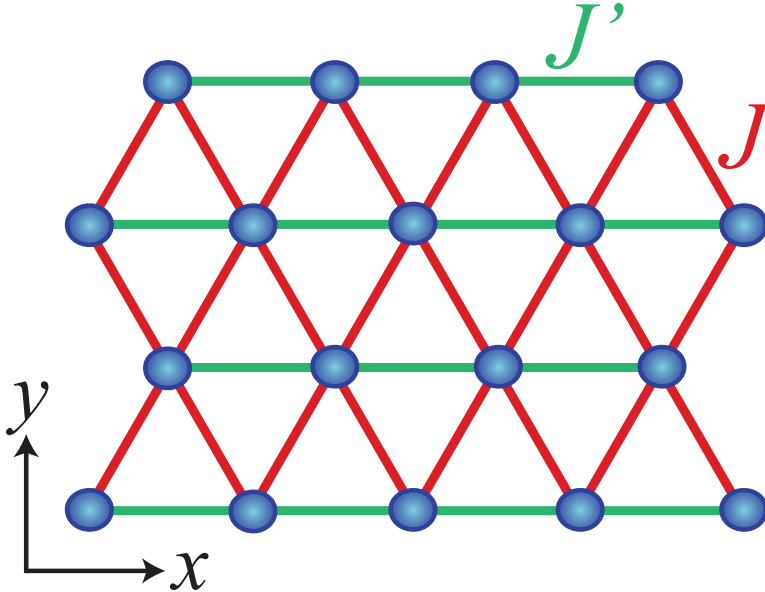


FIG. 1: Distorted triangular lattice with nearest-neighbor Heisenberg exchanges  $J'$  (on all horizontal bonds) and  $J$  (on all other bonds), representing the geometry of systems examined in this paper.

## I. INTRODUCTION

The study of exotic phases of quantum antiferromagnets has received a great impetus by the experimental discovery of a number of candidate  $S = 1/2$  Mott insulators. The primary aim of our paper is to present an attempt to place the experimentally discovered phases in a single global phase diagram; such a phase diagram exposes new relations between the excitations of the various phases, and leads to theories for the possible quantum phase transitions between them.

As will become clear from our analysis, we can generate distinct ‘global’ phase diagrams for distinct lattice types and exchange interactions in two spatial dimensions. We will present a general method for analyzing these, but will focus on a single lattice type, found in a number of experimental systems: this is the distorted triangular lattice shown in Fig. 1. Thus we are interested in the  $S = 1/2$  antiferromagnet, with  $SU(2)$  invariant Heisenberg exchange interactions  $J$  and  $J'$  illustrated in Fig. 1, along with possibly additional longer range two- or multi-spin exchange interactions which have the same symmetry as Fig. 1. A number of limiting cases of this lattice have been examined earlier, and we will connect with all of these results:

- (i) for  $J' \ll J$  the model becomes essentially equivalent to the square lattice antiferromagnets considered in Refs. 1,2,3, and our results agree with these earlier results in this regime;
- (ii) for  $J \ll J'$  we have the quasi-one dimensional antiferromagnets which have been studied

in some detail by Starykh and Balents<sup>4,5</sup>;

(iii) for  $J \approx J'$  we have the triangular lattice antiferromagnets for which our results will connect with those of Refs. 6,7,8,9;

(iv) Weihong, McKenzie and Singh<sup>10</sup> have performed a series expansion study for the entire range of  $J'/J$ , and obtained phases which will also appear in our phase diagrams;

(v) there have been a number of numerical studies<sup>11,12,13,14</sup> of isotropic triangular lattice case,  $J' = J$ , but with an additional four-spin ring exchange interaction, and our theory will provide candidate phase diagrams for this model; and

(vi) the non-magnetic phases for  $J' = J$  have been modeled by the quantum dimer model<sup>15</sup> on the triangular lattice by Moessner and Sondhi<sup>16</sup>, and our theory will also find their phases.

Experimental examples extend over the full range of parameters for the lattice in Fig. 1, and realize a variety of phases:

- A remarkable series of experiments have been carried out by R. Kato and collaborators<sup>17,18,19,20,21,22,23</sup> on the organic Mott insulators  $X[\text{Pd}(\text{dmit})_2]_2$  (for a general review of the organic compounds, see Ref. 24). Each site of the lattice in Fig. 1 has a pair of  $\text{Pd}(\text{dmit})_2$  molecules carrying charge  $-e$  and spin  $S = 1/2$ .  $X$  ranges over a variety of monovalent cations, and the choice of different  $X$  allows experiments over a range of values of  $J'/J$ . The resulting phase diagram<sup>22</sup> has magnetic order with decreasing critical temperatures from  $T_c \approx 42$  K to  $T_c \approx 15$  K across the compounds  $X = \text{Me}_4\text{P}$ ,  $\text{Me}_4\text{As}$ ,  $\text{EtMe}_3\text{As}$ ,  $\text{Et}_2\text{Me}_2\text{P}$ ,  $\text{Et}_2\text{Me}_2\text{As}$ , and  $\text{Me}_4\text{Sb}$ , as the value of  $J'/J$  increases from  $J'/J \approx 0.35$  to  $J'/J \approx 0.7$  (there are uncertainties in the overall scale of  $J'/J$ , and there are also likely to be significant four-spin ring exchange terms). The magnetic order is likely of the two-sublattice Néel type<sup>22</sup>, although there are no neutron scattering observations confirming this. The compound with  $X = \text{EtMe}_3\text{Sb}$  has  $J'/J \approx 0.85$  has no observable Néel order<sup>23</sup> and has been suggested to be near the quantum critical point<sup>22</sup> at which the Néel order vanishes. Finally, the compound<sup>20,21</sup> with  $X = \text{EtMe}_3\text{P}$  has  $J'/J \approx 1.05$  has a ground state with a spin gap and spontaneous columnar valence bond solid (VBS) order at low  $T$ . The VBS order vanishes at a phase transition observed to be at 25 K, and the low  $T$  spin gap is measured to be  $\approx 40$  K (the exchange constant  $J \approx 250$  K). Thus these series of compounds appear to realize the Néel-VBS transition predicted in Ref. 1, and in this paper we will place this transition in the context of global phase diagrams of models on the lattice of Fig. 1. We also note that a Néel-VBS transition as a function of increasing  $J'/J$  has also been found in the series expansion study<sup>10</sup>.
- A separate set of experiments have been performed on the organic Mott insulators  $\kappa\text{-(ET)}_2\text{Z}$ , which also realize the  $S = 1/2$  antiferromagnet on the lattice in Fig. 1. The compound with  $Z = \text{Cu}[\text{N}(\text{CN})_2]\text{Cl}$  has  $J'/J \approx 0.5$ , and has a ground state with Néel order<sup>25</sup>, as found in the  $\text{Pd}(\text{dmit})_2$  series above for small  $J'/J$ . The organic insulator with  $Z = \text{Cu}_2(\text{CN})_3$  has  $J'/J \approx 1$ , and appears to have no antiferromagnetic

or VBS ordering down to the lowest observed temperatures<sup>26,27,28,29</sup>. This is therefore a candidate for a spin liquid ground state, whose nature has been the subject of recent work<sup>13,30,31,32</sup>. The bosonic  $Z_2$  spin liquid state proposed for this compound in Ref. 32 will appear in our phase diagrams below, and indeed will be natural point of departure for our entire analysis. We believe the experimental observation, noted above, of the other phases in our phase diagram can be regarded as a point of support for our perspective. We will briefly mention below how  $Z_2$  spin liquid states with fermionic spinons<sup>30</sup>, and other related states, can appear in our approach.

- The transition metal insulator<sup>33,34</sup>  $\text{Cs}_2\text{CuCl}_4$  has  $S = 1/2$  Cu ions on the vertices of the triangular lattice in Fig. 1 with  $J \approx J'/3$ . The ground state has spiral antiferromagnetic order, similar to that present in the perfect triangular lattice ( $J = J'$ ), and as will appear in the phase diagrams below. An approach starting from the quasi one-dimensional limit  $J \ll J'$  has been successfully used<sup>4,5</sup> to describe the spiral ground state, and also the inelastic neutron scattering spectrum at high energies.

As noted above, our point of departure is a  $Z_2$  spin liquid state. The earliest proposals of such liquids involved BCS-like states of paired, charge 0,  $S = 1/2$  particles ('spinons') which were either bosons<sup>6</sup> or fermions<sup>35</sup>. Fluctuations about this state are expressed in terms of a  $Z_2$  gauge theory, in which the spinons carry a  $Z_2$  electric charge, and hence the name of the spin liquid. A large number of other models of  $Z_2$  spin liquids have appeared since<sup>16,36,37,38,39,40,41</sup>. We will find it convenient to begin with  $Z_2$  spin liquid in which the elementary spinons are bosons because it is connected naturally to a variety of ordered states found experimentally (which we have described above). We will denote the bosonic spinons by a complex field  $z_\alpha$ , where  $\alpha = \uparrow, \downarrow$  is a spin index.

Apart from the spinon, the other fundamental elementary excitation of a  $Z_2$  spin liquid is a charge 0 particle carrying  $Z_2$  magnetic flux. This particle was pointed out in Ref. 6, but its particular importance to the physical properties of  $Z_2$  spin liquids was emphasized by Senthil and Fisher<sup>36</sup>, who called it a 'vison'. In all cases we shall consider, it is possible to combine the real visons into complex scalar fields  $v_a$ , where  $a = 1 \dots N_v$  is an additional flavor index which depends upon the nature of the underlying lattice. The visons are bosons, but the spinons and visons have mutual semionic statistics<sup>36,42</sup>. Consequently, by forming bound states of the bosonic spinons,  $z_\alpha$ , and the visons,  $v_a$ , we obtain  $S = 1/2$  spinons which are fermions<sup>42</sup>. This bound state formation offers a route to extending our analysis to the case of fermionic spinons, but we shall not comment further on this in the present paper.

Our starting point is an effective field theory for the spinons,  $z_\alpha$ , and the visons,  $v_a$ , which implements their mutual semionic statistics. As discussed generally by Freedman *et al.*<sup>39</sup>, and implemented more specifically in  $Z_2$  spin liquids with fermionic spinons by Kou, Levin, and Wen<sup>43</sup>, this mutual statistics can be realized by a doubled U(1) Chern-Simons (CS) theory. A similar formalism was also applied to the cuprates, with a mutual statistics between spin and charge degrees of freedom<sup>44</sup>. To this end, we introduce 2 U(1) gauge fields,

$a_\mu$  and  $b_\mu$ , and will consider effective Lagrangians with the following schematic structure in 2+1 spacetime dimensions

$$\mathcal{L} = \sum_{\alpha=1}^2 \left\{ |(\partial_\mu - i a_\mu) z_\alpha|^2 + s_z |z_\alpha|^2 \right\} + \sum_{a=1}^{N_v} \left\{ |(\partial_\mu - i b_\mu) v_a|^2 + s_v |v_a|^2 \right\} + \frac{ik}{2\pi} \epsilon_{\mu\nu\lambda} a_\mu \partial_\nu b_\lambda + \dots, \quad (1.1)$$

where  $\mu, \nu, \lambda = x, y, \tau$  are spacetime indices, and  $s_z$  and  $s_v$  are the primary couplings we will tune to obtain our global phase diagrams. The integer  $k = 2$  implements the needed semionic statistics. The ellipses represent additional terms in the effective potential for the  $z_\alpha$  and  $v_a$  which are constrained by the projective symmetry group (PSG) *i.e.* the transformations of the spinons and visons under the symmetries of the lattice spin Hamiltonian. We will discuss these terms more carefully when we describe the different PSGs in the body of the paper.

In passing, we note that supersymmetric versions of the doubled Chern-Simons theory in Eq. (1.1) have recently been the focus of intense interest in the string theory literature<sup>45,46,47,48,49,50</sup>. Their model of interest is<sup>47</sup> a Chern-Simons theory with a  $U(N) \times U(N)$  gauge group, with opposite signs for the Chern-Simons term for the two  $U(N)$ 's, and with matter fields which are bifundamentals in the  $U(N)$ s. Eq. (1.1) is also precisely of this form with  $N = 1$ : we can define  $c_\mu = a_\mu + b_\mu$  and  $d_\mu = a_\mu - b_\mu$ , and then the  $c_\mu$  and  $d_\mu$  fields have diagonal Chern-Simons terms with opposite signs, and the  $z_\alpha$  and  $v_a$  carry bifundamental charges. The  $U(N) \times U(N)$  theories have been argued<sup>48,49</sup> to be dual to M theory on  $AdS_4 \times S^7/Z_k$ , which is reason for the interest. The  $N = 1$  case with  $\mathcal{N} = 4$  supersymmetry has been argued<sup>50</sup> to be exactly dual to a  $U(1)$  gauge theory without a Chern-Simons terms (the latter theory was reviewed in Ref. 51). The analogs of such  $N = 1$  dualities for non-supersymmetric theories are well-known in the condensed matter literature, and we will discuss examples in the present paper (see also Ref. 36).

A natural question arises at this point: what are the conditions under which it is permissible to implement a  $U(1)$  CS theory realization of the  $Z_2$  spin liquid, rather than directly in terms of a  $Z_2$  gauge theory? When we are discussing the topological properties of the ground state, or about single quasiparticle excitations, there does not appear to be any obstacle to using a  $U(1)$  theory<sup>43</sup>. However, the issue becomes more delicate when the excitations proliferate, and we are considering quantum phase transitions out of the spin liquid state. This question is discussed further in Section VI, where we will find examples of transitions at which our  $U(1)$  CS description fails. However, we also find cases where it does succeed, and these are the main focus of this paper. As we will see in Section IV, for these successful cases, because of the constraints of the lattice PSG, the lowest order terms which break either of the  $U(1)$  gauge invariances of Eq. (1.1) are of eighth order,  $\sim v_a^8$  as in Eq. (4.2); their effects are easily incorporated into our analysis as a soft symmetry breaking. We mention that the connection between doubled  $Z_2$  and  $U(1)$  CS theories has also been discussed by Balents and Fisher in a different context<sup>52</sup>.

Crucial to our analysis will be exact results on the low energy spectrum of  $\mathcal{L}$  on a  $L \times L$  torus as a function of  $s_z$  and  $s_v$ . For the case where both  $s_v$  and  $s_z$  are large and positive, both the spinons and visons are gapped, and we realize a  $Z_2$  spin liquid. Here we can integrate out the  $z_\alpha$  and  $v_a$ , and are left with a pure doubled Chern-Simons (CS) gauge theory. This theory was quantized exactly on a torus in Refs. 39,43. The key variables in this quantization were the fluxes piercing the two cycles,  $C_{x,y}$  of the torus

$$A_i = \oint_{C_i} a_\mu dx_\mu \quad , \quad B_i = \oint_{C_i} b_\mu dx_\mu. \quad (1.2)$$

Given that all the matter fields carry unit  $a_\mu$  or  $b_\mu$  charges, the  $A_i$  and  $B_i$  should be regarded as periodic variables taking values on a circle of circumference  $2\pi$ . After accounting for this periodicity, The solution of the ground state of the CS theory was found to be 4-fold degenerate; the degeneracy appears exponentially fast as  $L \rightarrow \infty$ , provided the vison and spinon gaps remain finite. This 4-fold degeneracy is viewed as an essential characterization of the  $Z_2$  spin liquid<sup>6,42</sup>.

The other phases in our phase diagrams appear when we allow one or both of  $s_z$  and  $s_v$  to vary to negative values. Then we can have phase transitions to new phases in which one or both of the  $z_\alpha$  and  $v_a$  are “condensed”. However, the precise nature of the broken symmetry, if any, is not immediately obvious in such phases, given the presence of the 2 gauge fields and their CS term. The purpose of this paper is to describe these new phases and the associated quantum critical points. Here we note that the order parameter characterizing these states can be gleaned by carefully examining the low energy states of  $\mathcal{L}$  on a  $L \times L$  torus. As an example, consider the state where  $s_z$  is large and negative, and so a saddle point with  $z_\alpha \neq 0$  is favored. By global  $SU(2)$  spin symmetry, there are actually an infinite number of such saddle points along the manifold  $|z_\uparrow|^2 + |z_\downarrow|^2 = \text{constant}$  *i.e.* along  $S^3$ , the surface of a sphere in four dimensions. The low energy theory on a  $L \times L$  torus can be expressed as a functional integral over  $S^3$ , along with an integral over the gauge fields. We will solve this quantum theory exactly, and find an “Anderson tower of states”<sup>56</sup>, with a non-degenerate ground state, and an infinite sequence of excited levels with energies  $\sim 1/L^2$  above the ground state energy. The sequence of excited levels, and their degeneracies, can be uniquely identified with the quantum mechanics of a particle moving on  $S^3/Z_2$ , with the co-ordinates of the particle representing the average orientation of the order parameter across the entire torus. In other words, the primary effect of the gauge fluctuations is to reduce the order parameter characterizing the broken symmetry from  $S^3$  to  $S^3/Z_2$ . It was these same gauge fluctuations which were responsible for the 4-fold degeneracy in the  $Z_2$  spin liquid. The  $S^3/Z_2 \cong SO(3)$  order parameter allows an immediate identification of the  $s_z$  large and negative state: this is the spiral antiferromagnet, as found in  $\text{Cs}_2\text{CuCl}_4$ .

A related analysis for the other phases will be found in the body of the paper, allowing us to construct our phase diagrams. Here we show in Fig. 2 the phase diagram found for a case

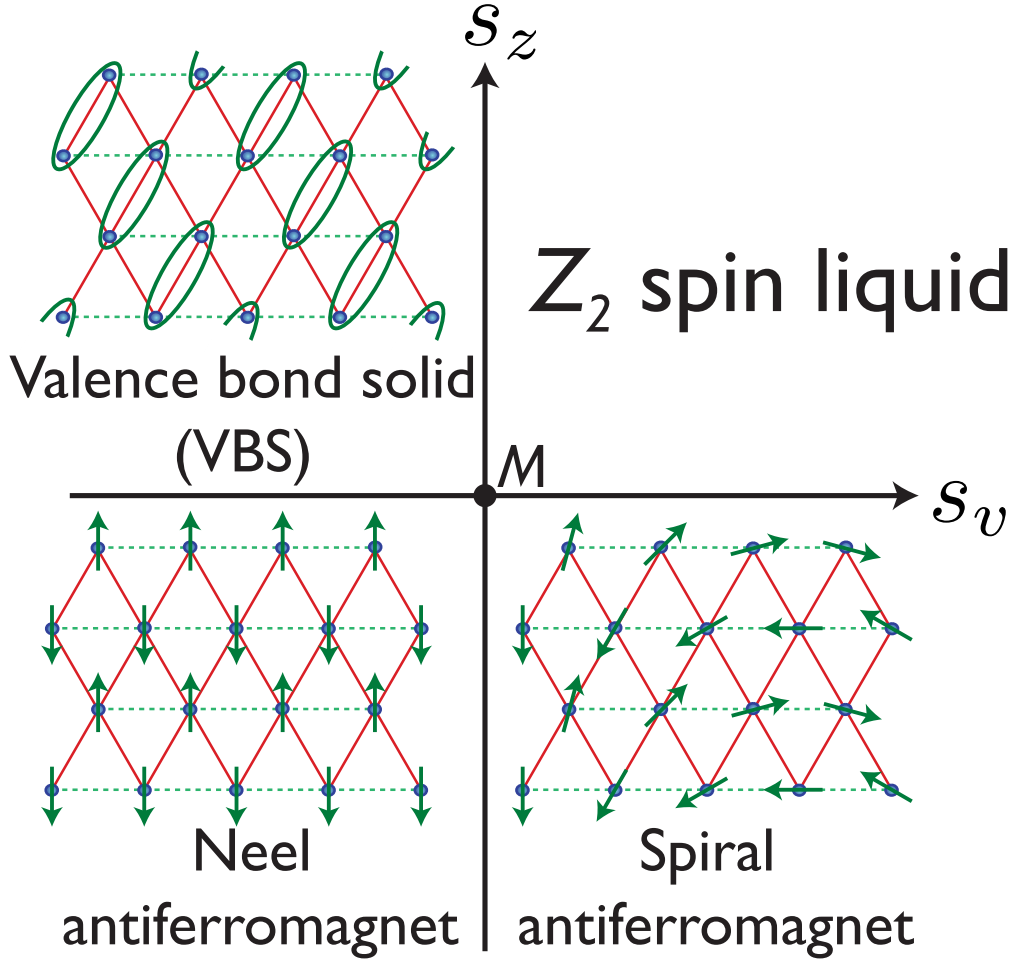


FIG. 2: Global phase diagram for the case with  $N_v = 1$  and a particular model of the spinons (model BIII); a similar phase diagram appeared in Ref. 8. The Néel antiferromagnet is found in a many materials, and has ordering wavevector  $\mathbf{Q} = 2\pi(1, 0)$ . The geometry of the VBS state coincides with that found<sup>20,21</sup> in  $\text{EtMe}_3\text{P}[\text{Pd}(\text{dmit})_2]_2$ . The spiral antiferromagnet shown in the figure has an ordering wavevector  $\mathbf{Q} = 2\pi(1 - \epsilon, 0)$  with  $\epsilon = 1/6$ , small, as expected for  $J' < J$ . The experimentally realized spiral state in  $\text{Cs}_2\text{CuCl}_4$  has  $J' > J$ , and consequently a larger value of  $\epsilon \approx 1/2$ . The  $Z_2$  spin liquid in this phase diagram is similar to that proposed in Ref. 32 to explain observations<sup>26,27,28,29</sup> in  $\kappa\text{-(ET)}_2\text{Cu}_2(\text{CN})_3$ . The transitions have been discussed previously: (i) the  $\text{CP}^1$  field theory for the Néel-VBS transition<sup>3</sup>, (ii) the  $\text{O}(4)$  field theory for the spiral- $Z_2$  spin liquid transition<sup>53,54,55</sup>, (iii) the mean field theory for the spiral-Néel transition<sup>8</sup>, and (iv) the  $\text{O}(2)$  field theory for the VBS- $Z_2$  spin liquid transition<sup>7,16</sup>. All these field theories are contained in our theory in Eq. (1.1), which also describes the multicritical point M.

in which there is only one vison flavor,  $N_v = 1$  and for a particular model of the spinons—we label this theory model BIII. A mean-field phase diagram with the same phases appeared already in Ref. 8, and here we shall show that these phases follow from the very general considerations outlined above, and also provide field theories for all the transitions and the



multicritical point  $M$ . It is encouraging that all the phases with broken symmetry, which descend from the  $Z_2$  spin liquid with  $N_v = 1$ , correspond precisely to those which have been experimentally observed so far.

In Section II we will describe the phase diagram of the theory in Eq. (1.1) as an abstract field theory, without reference to any underlying antiferromagnet. The specific spinon and vison degrees of freedom of the lattice antiferromagnet, and their possible PSGs, will be identified in Section III. The combination of the results of Sections II and III lead to a variety of possible phase diagrams. These are described in Section IV, and the quantum phase transitions in Section V. Section VI will give another semiclassical perspective on our results, which also identifies the limitations of the present U(1) CS approach. The concluding Section VII will make some further remarks on recent experiments.

## II. PHASES OF THE DOUBLED CHERN-SIMONS THEORY

This section will discuss the phase diagram of the doubled CS theory, considered here as an abstract field theory. The interpretation of the phases in terms of the underlying antiferromagnet requires a more specific knowledge of the PSGs of the spinons and visons, and these will be considered in subsequent sections.

For the case where the spinons and visons are gapped, as we have already noted, we obtain the  $Z_2$  spin liquid. The fundamental property of this theory is the 4-fold degeneracy on a  $L \times L$  torus, and this appears as a property of the pure doubled CS theory<sup>39,43</sup>. We are now interested in moving into one of the phases where one or both of the spinons and visons are “condensed” and understanding the nature of the broken symmetry. As in the  $Z_2$  spin liquid, we will do this here by examining the low energy states of the theory on the  $L \times L$  torus. We will compute the spectrum of Anderson’s<sup>56</sup> “tower of states” with excitation energies  $\sim 1/L^2$ : the spectrum of states will allow a unique identification of the ground state manifold (GSM) associated with the broken global symmetry.

We will only consider here the case where there is a single spinon species,  $z$ , and a single vison species  $v$ ; the generalization to the multiple species case is straightforward. For the broken symmetry phases, we need only consider the phases of these complex fields, and so we will write  $z \sim e^{i\theta_z}$  and  $v \sim e^{i\theta_v}$  where the corresponding symmetries are broken.

As a warmup, consider first the case with a single broken U(1) symmetry, characterized by the U(1) order parameter  $e^{i\theta}$ , and no gauge fields. The low energy theory of  $\theta$  fluctuations is given by the action

$$\mathcal{S}_\theta = \int d^2r d\tau \left[ \frac{K_1}{2} (\partial_\tau \theta)^2 + \frac{K_2}{2} (\partial_i \theta)^2 \right], \quad (2.1)$$

on a  $L \times L$  torus, with  $\theta$  and  $\theta + 2\pi$  identified. The couplings  $K_{1,2}$  are two stiffnesses characterizing the broken symmetry. Because this is a Gaussian theory, we can make the

mode expansion

$$\theta(x, y, \tau) = \theta_0(\tau) + \frac{2\pi m x}{L} + \frac{2\pi n y}{L} + \frac{1}{L} \sum_{k \neq 0} a_k(\tau) e^{ik \cdot r} \quad (2.2)$$

where  $n$  and  $m$  are fixed integers (the winding numbers),  $\theta_0$  represents the uniform fluctuation of the order parameter, and the  $a_k$  are the ‘spin-wave’ normal modes. Inserting this in the action we obtain

$$\mathcal{S}_\theta = 4\pi^2(m^2 + n^2) + \int d\tau \left[ \frac{K_1 L^2}{2} (\partial_\tau \theta_0)^2 + \sum_{k \neq 0} \left( \frac{K_1}{2} (\partial_\tau a_k)^2 + \frac{K_2}{2} k^2 a_k^2 \right) \right] \quad (2.3)$$

From this it is clear that the low-lying states have  $m = n = 0$ . The  $a_k$  harmonic oscillators have energy  $\sim k \sim 1/L$ , while the  $\theta_0$  mode has energy  $\sim 1/L^2$ . So for the lowest states, we put all the  $a_k$  oscillators in the ground state, and we obtain a tower of states with energy

$$E_p = E_0 + \frac{p^2}{2K_1 L^2} \quad (2.4)$$

where  $p$  is an integer, measuring the angular momentum of the  $\theta_0$  mode.

It is now useful to note that the theory  $\mathcal{S}_\theta$  in Eq. (2.1) is exactly dual to U(1) gauge theory with a Maxwell term, and so the latter should have the same tower of low energy states. Let us demonstrate this explicitly. First, we decouple the quadratic terms in Eq. (2.1) by an auxiliary current  $J_\mu$

$$\mathcal{S}_\theta = \int d^2 r d\tau \left[ \frac{J_\tau^2}{2K_1} + \frac{J_i^2}{2K_2} + i J_\mu \partial_\mu \theta \right], \quad (2.5)$$

Integrating over  $\theta$ , we obtain the constraint  $\partial_\mu J_\mu = 0$ , which we solve by expressing  $J_\mu$  in terms of a ‘dual’ gauge field  $a_\mu$ :

$$J_\mu = \frac{1}{2\pi} \epsilon_{\mu\nu\lambda} \partial_\nu a_\lambda. \quad (2.6)$$

The normalization of  $1/(2\pi)$  is chosen so that periodicity of the flux variables  $A_i$  in Eq. (1.2) with period  $2\pi$  is equivalent to the periodicity in the angular variable  $\theta \rightarrow \theta + 2\pi$ . Now inserting Eq. (2.6) into (2.5) we obtain the U(1) gauge theory dual to  $\mathcal{S}_\theta$ :

$$\mathcal{S}_a = \int d^2 r d\tau \left[ \frac{1}{8\pi^2 K_2} (\partial_\tau a_i)^2 + \frac{1}{8\pi^2 K_1} (\partial_x a_y - \partial_y a_x)^2 \right] \quad (2.7)$$

where we have chosen the temporal gauge with  $a_\tau = 0$ . An important consequence of the periodicity in  $A_i$  variables is that the flux piercing the torus,  $\int d^2 r (\partial_x a_y - \partial_y a_x)$  must be an integer multiple of  $2\pi$ . We can see this by moving the contour  $C_i$  in Eq. (1.2) across the entire length of the torus: the change in the line integral upon returning to the initial

position must be an integer multiple of  $2\pi$ , and this change is equal by Stokes theorem to the flux piercing the torus. Thus the Hilbert space of  $\mathcal{S}_a$  breaks apart into distinct sectors with total flux  $2\pi p$ , where  $p$  is an integer. Within each sector, the ground state has zero photons (which are the dual of the spin waves), and has  $\langle \partial_x a_y - \partial_y a_x \rangle = (2\pi p)/L^2$ . So the lowest energy state in each sector is

$$E_p = E_0 + \frac{L^2}{8\pi^2 K_1} \left( \frac{2\pi p}{L^2} \right)^2 = E_0 + \frac{p^2}{2K_1 L^2} \quad (2.8)$$

which is the same as the spectrum of  $S_\theta$  in Eq. (2.4). This verifies the equivalence of Eq. (2.1) and (2.7).

With these preliminaries out of the way, let us return to our doubled CS theory with one spinon and one vison. Consider the phase where the spinon is condensed and the vison is gapped, so  $s_v \gg 0$  and  $s_z \ll 0$ . Here we can simply integrate out the vison, and are left with the following low energy theory for  $\theta_z$  and the  $U(1)$  gauge fields

$$\mathcal{S}_z = \int d^2 r d\tau \left[ \frac{K_1}{2} (\partial_\tau \theta_z - a_\tau)^2 + \frac{K_2}{2} (\partial_i \theta_z + a_i)^2 + \frac{ik}{2\pi} a_\mu \epsilon_{\mu\nu\lambda} \partial_\nu b_\lambda \right] \quad (2.9)$$

We can always choose the gauge  $\theta_z = 0$  (and  $A_\tau = 0$ ). In this gauge, the integral over  $a_\mu$  is an ordinary Gaussian. Performing this integral, we obtain the action

$$\mathcal{S}_z = \int d^2 r d\tau \left[ \frac{k^2}{8\pi^2 K_2} (\partial_\tau b_i)^2 + \frac{k^2}{8\pi^2 K_1} (\partial_x b_y - \partial_y b_x)^2 \right] \quad (2.10)$$

Comparing this with the spectrum of  $\mathcal{S}_a$  in Eq. (2.8), we obtain the low-lying states

$$E_p = E_0 + \frac{k^2 p^2}{2K_1 L^2} \quad (2.11)$$

This shows that the theory  $\mathcal{S}_z$  in Eq. (2.9) is equivalent to the  $U(1)$  scalar theory in Eq. (2.1) but with the periodicity  $\theta \equiv \theta + 2\pi/k$ . In other words, the GSM of this phase has been modified by the gauge fluctuations from  $S^1$  to  $S^1/Z_k$ . Alternatively stated, the broken symmetry of the ground state is associated with distinct values of the composite field  $z^k$ .

It is useful to have another perspective on the above result by an alternative analysis of the theory  $\mathcal{S}_z$  in Eq. (2.9). This analysis begins by ‘undualizing’ the gauge field  $b_\mu$  into a dual scalar  $\theta_b$ . For this we introduce, as in Eq. (2.6), the current  $J_\mu^b = \epsilon_{\mu\nu\lambda} \partial_\nu b_\lambda / (2\pi)$  and impose the constraint  $\partial_\mu J_\mu^b = 0$  by a Lagrange multiplier  $\theta_b$ ; this modifies  $\mathcal{S}_z$  in Eq. (2.9) to

$$\mathcal{S}_z = \int d^2 r d\tau \left[ \frac{K_1}{2} (\partial_\tau \theta_z - a_\tau)^2 + \frac{K_2}{2} (\partial_i \theta_z + a_i)^2 + i J_\mu^b (k a_\mu - \partial_\mu \theta_b) + \frac{J_\mu^{b2}}{2\tilde{K}} \right] \quad (2.12)$$

The last term is a useful regularization, and the original theory in Eq. (2.9) is obtained in

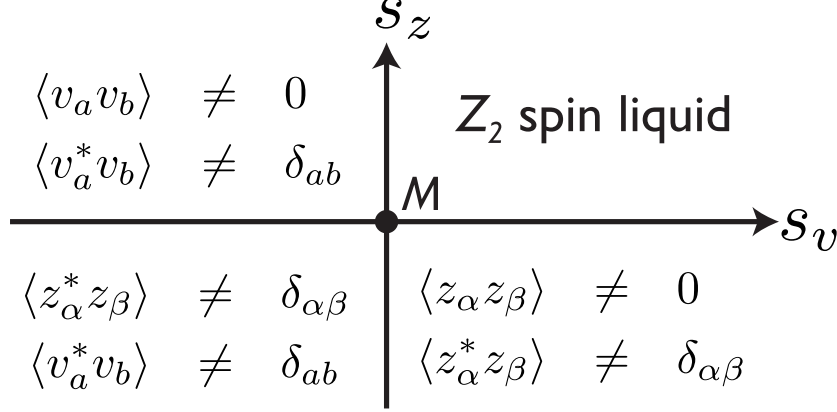


FIG. 3: Schematic phase diagram of the doubled CS theory in Eq. (1.1) for  $k = 2$ . All non-zero order parameters which characterize the broken symmetry in each phase are shown.

the limit  $\tilde{K} \rightarrow \infty$ . Now we perform the integral over  $J_\mu^b$  and obtain the theory

$$\mathcal{S}_z = \int d^2r d\tau \left[ \frac{K_1}{2} (\partial_\tau \theta_z - a_\tau)^2 + \frac{K_2}{2} (\partial_i \theta_z + a_i)^2 + \frac{\tilde{K}}{2} (k a_\mu - \partial_\mu \theta_b)^2 \right] \quad (2.13)$$

In the limit  $\tilde{K} \rightarrow \infty$ , we see that we must have  $a_\mu = (1/k) \partial_\mu \theta_b$ . However,  $\theta_b$  is a variable periodic under  $\theta_b \rightarrow \theta_b + 2\pi$ , and hence the periodic flux variables  $A_i$  in Eq. (1.2) can only take the values

$$A_i = \frac{2\pi p_i}{k} \quad (2.14)$$

where the  $p_i$  are integers. In other words,  $U(1)$  gauge field  $a_\mu$  has been reduced to a  $Z_k$  gauge field. Thus  $e^{ik\theta} \sim z^k$  is gauge invariant, and this explains our results above on the distinct values of  $z^k$  identifying distinct ground states.

We have now completed our discussion of the state where the spinon is condensed and the vison is gapped ( $s_v \gg 0$  and  $s_z \ll 0$ ). Clearly, the complementary phase where the vison is condensed and the spinon is gapped ( $s_v \ll 0$  and  $s_z \gg 0$ ) is amenable to a parallel treatment, with complementary results and a  $v^k$  order parameter.

Finally, let us consider the case where both the visons and spinons are condensed,  $s_v \ll 0$  and  $s_z \ll 0$ . In this case, we can see in the gauge  $\theta_z = 0$  and  $\theta_v = 0$  that both fields  $a_\mu$  and  $b_\mu$  are fully gapped. So there is a unique ground state, and no other excited states whose energy vanishes as  $L \rightarrow \infty$ .

We can now generalize these results to the cases with multiple flavors of visons and spinons, and the results are summarized in Fig. 3 for  $k = 2$ . The flavor indices simply tag along for the order parameters involving a  $k$ -fold composites of spinons or visons, which are invariant under the  $Z_k$  gauge transformations. However, there are now also additional gauge-neutral order parameters possible, like  $z_\alpha^* z_\beta$ , which were absent for the single flavor

case, because they were not associated with any broken symmetry.

Armed with the results in Fig. 3, and with a knowledge of the microscopic PSGs of the spinons and visons (which are described next in Section III), we can easily deduce the physical characteristics of the phases of a variety of antiferromagnets.

### III. SPINONS AND VISONS

A rich variety of spinon and vison operators can be defined for  $S = 1/2$  antiferromagnets on the lattice in Fig. 1, and we shall not attempt any complete classification. Clearly, the choice depends sensitively on the details of the microscopic Hamiltonian. However, in previous semiclassical analyses, a few natural choices have emerged for different limiting values of  $J'/J$ . We will describe these below, and show how they can fit together in a doubled CS theory like Eq. (1.1).

The essential characteristics of the spinons and visons will be their transformations under the symmetry operations of the underlying spin model. These symmetries are the lattice translations  $T_1$  and  $T_2$ , the lattice reflections  $P_x$  and  $P_y$ , and time reversal,  $T$ :

$$\begin{aligned} T_1 &: (x, y) \rightarrow (x + 1, y) \\ T_2 &: (x, y) \rightarrow (x + 1/2, y + \sqrt{3}/2) \\ P_x &: (x, y) \rightarrow (-x, y) \\ P_y &: (x, y) \rightarrow (x, -y) \\ T &: t \rightarrow -t \end{aligned} \tag{3.1}$$

Spin rotation is also a symmetry, and is easily implemented by contracting the spinor indices.

The following subsections will consider the PSGs of spinons and visons in turn.

#### A. Spinons

One natural model of spinons appears upon describing the spiral ground state of the triangular lattice antiferromagnet in terms of Schwinger bosons. So we write the spin operator on the lattice sites as  $\vec{S} = b^\dagger \vec{\sigma} b / 2$ , where  $\vec{\sigma}$  are the Pauli matrices. For the Schwinger bosons we make the following low energy expansion<sup>57</sup> in terms of the spinon fields,  $z_\alpha$ :

$$b_\alpha \sim z_\alpha \exp(i\mathbf{Q} \cdot \mathbf{r}/2) + i\epsilon_{\alpha\beta} z_\beta^* \exp(-i\mathbf{Q} \cdot \mathbf{r}/2), \tag{3.2}$$

From this parameterization we can then deduce the following expression for the spin operators

$$\vec{S} = \vec{n}_1 \cos(\mathbf{Q} \cdot \mathbf{r}) + \vec{n}_2 \sin(\mathbf{Q} \cdot \mathbf{r}),$$

$$\begin{aligned}
\vec{n}_1 &= \text{Re}[z^t \sigma^y \vec{\sigma} z], \quad \vec{n}_2 = \text{Im}[z^t \sigma^y \vec{\sigma} z], \\
\vec{n}_3 &= \vec{n}_1 \times \vec{n}_2 = z^\dagger \vec{\sigma} z.
\end{aligned}
\tag{3.3}$$

We observe that  $\mathbf{Q}$  is the ordering wavevector of the spiral. So for  $J' \approx J$ , we expect  $\mathbf{Q} \approx (2\pi/3, 0)$ . For  $\text{Cs}_2\text{CuCl}_4$ , which has  $J' \approx 3J$ , we have  $\mathbf{Q} \approx (\pi, 0)$ . Finally, in the square lattice limit,  $J' \ll J$ , we have  $\mathbf{Q} \approx (2\pi, 0)$ . Thus we expect  $\mathbf{Q}$  to increase monotonically from  $(\pi, 0)$  to  $(2\pi, 0)$  with decreasing  $J'/J$ . Also note that  $\vec{n}_{1,2,3}$  are three mutually orthogonal vectors.

The parameterization in Eq. (3.3) allows us to deduce the PSG of the  $z_\alpha$ . These  $z_\alpha$  spinons will couple minimally to the  $a_\mu$  gauge field, and so there is a natural implied PSG for the  $a_\mu$ . We call the resulting PSG of spinons as model A:

$$\begin{aligned}
&\text{Spinons, Model A} \\
T_1 : z &\rightarrow e^{iQ_x/2} z, \quad a_\mu \rightarrow a_\mu \\
T_2 : z &\rightarrow e^{iQ_x/4} z, \quad a_\mu \rightarrow a_\mu \\
P_x : z_\alpha &\rightarrow \epsilon_{\alpha\beta} z_\beta^*, \quad a_x \rightarrow a_x, \quad a_y \rightarrow -a_y, \quad a_t \rightarrow -a_t \\
P_y : z &\rightarrow z, \quad a_x \rightarrow a_x, \quad a_y \rightarrow -a_y, \quad a_t \rightarrow a_t \\
T : z &\rightarrow iz^*, \quad a_\mu \rightarrow a_\mu.
\end{aligned}
\tag{3.5}$$

We note that under this model A PSG,  $\vec{n}_{1,2}$  are odd under time reversal, while  $\vec{n}_3$  is even. From this, and the representation in Eq. (3.3), we deduce that  $\vec{n}_3$  is a spin nematic order parameter.

The Model A spinons are natural for  $J' \gtrsim J$ , where the spiral order is likely to be present. However as we approach the square lattice limit with  $J' \rightarrow 0$ , there is a finite range of small  $J' < J$  over which we expect that  $\mathbf{Q}$  is pinned exactly at  $(2\pi, 0)$ , and we have the conventional 2 sublattice Néel order appropriate for the square lattice. In this case  $\sin(\mathbf{Q} \cdot \mathbf{r}) = 0$  identically, and  $\cos(\mathbf{Q} \cdot \mathbf{r}) = \cos(2\pi x) = (-1)^{2x}$ . In this limit, we can define another model of spinons which appeared in previous theories of square lattice antiferromagnets<sup>1,2</sup>. We map  $z_\alpha \rightarrow (z_\alpha + i\epsilon_{\alpha\beta} z_\beta^*)/\sqrt{2}$  and then find that Eq. (3.3) is replaced by

$$\vec{S} = \vec{m}_1 (-1)^{2x}, \quad \vec{m}_1 = z^\dagger \vec{\sigma} z,
\tag{3.6}$$

A significant difference from Eq. (3.3) is that now the U(1) gauge invariance associated with  $a_\mu$  is explicit, because the representation (3.6) is invariant under the gauge transformation  $z_\alpha \rightarrow z_\alpha e^{i\theta}$ . We label these spinons model B, and they also have mappings under the square lattice space group, which we can deduce from Eq. (3.6) to be:

$$\begin{aligned}
&\text{Spinons, Model B} \\
T_1 : z &\rightarrow -z, \quad a_\mu \rightarrow a_\mu
\end{aligned}
\tag{3.7}$$

$$\begin{aligned}
T_2 &: z_\alpha \rightarrow -\epsilon_{\alpha\beta} z_\beta^*, \quad a_\mu \rightarrow -a_\mu \\
P_x &: z \rightarrow iz, \quad a_x \rightarrow -a_x, \quad a_y \rightarrow a_y, \quad a_t \rightarrow a_t \\
P_y &: z \rightarrow z, \quad a_x \rightarrow a_x, \quad a_y \rightarrow -a_y, \quad a_t \rightarrow a_t \\
T &: z_\alpha \rightarrow \epsilon_{\alpha\beta} z_\beta, \quad a_\mu \rightarrow -a_\mu.
\end{aligned} \tag{3.8}$$

It is now clear that under the model B PSG,  $\vec{m}_1$  is odd under time-reversal. In the state where the spinons are condensed and the visons are gapped, we see from Fig. 3 that we also have two additional vectors in spin space which characterize the broken symmetry in the ground state (analogous to the 3 vectors found in model A):

$$\vec{m}_2 + i\vec{m}_3 = z^t \sigma^y \vec{\sigma} z \tag{3.9}$$

These vectors do not appear in the present expression for the spin operator in Eq. (3.6), and so their physical interpretation is not yet clear. Let us, therefore, compute the PSG of these vectors:

$$\underline{\text{Model B}} \tag{3.10}$$

$$\begin{aligned}
T_1 &: \vec{m}_{2,3} \rightarrow \vec{m}_{2,3} \\
T_2 &: \vec{m}_2 \rightarrow \vec{m}_2, \quad \vec{m}_3 \rightarrow -\vec{m}_3 \\
P_x &: \vec{m}_{2,3} \rightarrow -\vec{m}_{2,3} \\
P_y &: \vec{m}_{2,3} \rightarrow \vec{m}_{2,3} \\
T &: \vec{m}_2 \rightarrow \vec{m}_2, \quad \vec{m}_3 \rightarrow -\vec{m}_3
\end{aligned} \tag{3.11}$$

From these properties it is evident that we can identify  $\vec{m}_2$  as the central axis (in spin space) about which the spins are precessing in the spiral antiferromagnet shown in Fig. 2. We will present a more detailed analysis in Section IV D which shows how the spiral state emerges for model B spinons. This identification is also consistent with the analysis of this phase in Ref. 8, where the spiral phase was induced by the condensation of a charge 2 Higgs scalar—the vison is dual to this scalar, and the gapping of the vison is equivalent to the condensation of the Higgs scalar.

## B. Visons

In the simplest models of visons<sup>7,16,36</sup>, we take real particles hopping on the sites of the dual lattice, subject to a flux of  $\pi$  around every site of the direct lattice. In other words, the vison is the Ising field of an Ising model on the dual lattice, with exchange couplings chosen so that every plaquette surrounding a direct lattice site is frustrated. For the antiferromagnet on the lattice in Fig. 1, the Ising model resides on the dual lattice shown in Fig. 4. Because of the dual relation between the couplings of the antiferromagnet, and the model of the visons, we expect that  $w'/w$  decreases as  $J'/J$  increases.

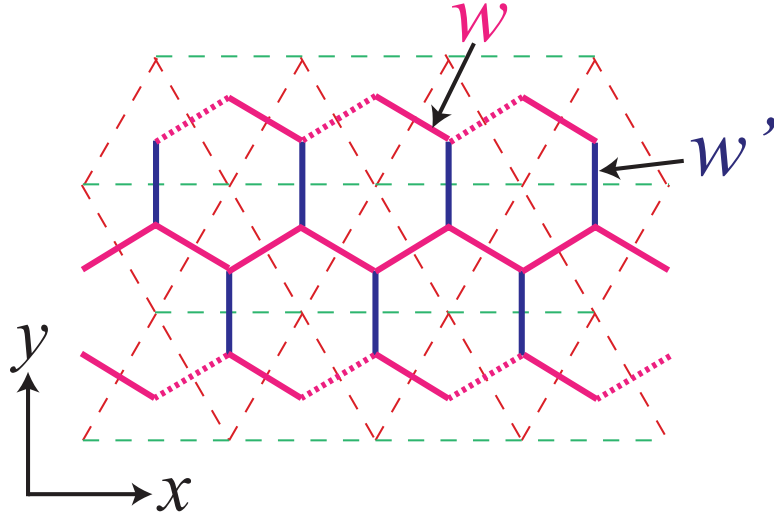


FIG. 4: The dual Ising model describing the vison dynamics in the dual honeycomb lattice. All the vertical bonds have hopping amplitude  $w'$ , all the other bonds have hopping amplitude  $w$ . Note that a small  $J'/J$  implies a large  $w'/w$ , and vice versa. Besides the lattice anisotropy, there is a  $\pi$ -flux through every hexagon, which frustrates the vison kinetics; this flux is implemented by changing the sign of the dotted  $w$  bonds.

It is a relatively straightforward matter to obtain the spectrum of such a particle moving on the lattice in Fig. 4. Because the kinetics of the vison is frustrated by the background spinon charge on every site, the product of the hopping amplitudes on the six links around each hexagon is -1. We are free to choose one of the links to be negative, and our convention is shown in Fig. 4. The spectrum has multiple minima in the Brillouin zone, and we introduce a real vison field for each such minimum in the spectrum. This procedure parallels that carried out in obtaining the multiple vortex flavors in Refs. 58 and 59, but with modification that we are considering real vison fields and not complex vortex fields.

For the general set of parameters for the lattice in Fig. 4, we find that there are either 4 or 2 minima of the vison dispersion lattice in the Brillouin zone. The 4 minima occur near  $J' \approx J$ , and so are appropriate for the triangular lattice limit; indeed for  $J' = J$  these minima co-incide with those found by Moessner and Sondhi<sup>16</sup>. For  $J'/J$  small ( $w'/w$  large), near the square lattice limit, we find only 2 minima.

Let us begin by considering the 4 minima case. These are at momenta of the form

$$\begin{aligned}
 \mathbf{q}_1 &= (q_{1x}, \pi/2), \\
 \mathbf{q}_2 &= (\pi - q_{1x}, \pi/2), \\
 \mathbf{q}_3 &= (-q_{1x}, -\pi/2), \\
 \mathbf{q}_4 &= (q_{1x} - \pi, -\pi/2).
 \end{aligned} \tag{3.12}$$



There are two choices to combine these four real minima to two complex minima, which will then correspond to the complex vison fields  $v_a$ , with  $a = 1, 2$ . The first choice, which we call model I, is:

$$\begin{aligned} v_1 : \mathbf{q}_1 &= (q_{1x}, \pi/2), \\ v_2 : \mathbf{q}_2 &= (\pi - q_{1x}, \pi/2), \\ v_1^* : \mathbf{q}_3 &= (-q_{1x}, -\pi/2), \\ v_2^* : \mathbf{q}_4 &= (q_{1x} - \pi, -\pi/2), \end{aligned} \quad (3.13)$$

while model II is:

$$\begin{aligned} v_1 : \mathbf{q}_1 &= (q_{1x}, \pi/2), \\ v_2^* : \mathbf{q}_2 &= (\pi - q_{1x}, \pi/2), \\ v_1^* : \mathbf{q}_3 &= (-q_{1x}, -\pi/2), \\ v_2 : \mathbf{q}_4 &= (q_{1x} - \pi, -\pi/2). \end{aligned} \quad (3.14)$$

These two choices lead to 2 models for the vison PSGs:

$$\begin{aligned} &\text{Visons, Model I} \\ T_1 : v_1 &\rightarrow e^{iq_{1x}} v_1, \quad v_2 \rightarrow e^{i\pi - iq_{1x}} v_2, \quad b_\mu \rightarrow b_\mu \\ T_2 : v_1 &\rightarrow e^{i\theta} v_2^*, \quad v_2 \rightarrow -ie^{-i\theta} v_1^*, \quad b_\mu \rightarrow -b_\mu \\ P_x : v_1 &\rightarrow e^{-i\gamma} v_1^*, \quad v_2 \rightarrow -e^{i\gamma} v_2^*, \quad b_x \rightarrow b_x, \quad b_y \rightarrow -b_y, \quad b_t \rightarrow -b_t \\ P_y : v_1 &\rightarrow v_2^*, \quad v_2 \rightarrow v_1^*, \quad b_x \rightarrow -b_x, \quad b_y \rightarrow b_y, \quad b_t \rightarrow -b_t \\ T : v_a &\rightarrow v_a^*, \quad b_\mu \rightarrow b_\mu \end{aligned} \quad (3.15)$$

where  $\gamma$  and  $\theta$  are two incommensurate angles.

The second model for the vison PSG is

$$\begin{aligned} &\text{Visons, Model II} \\ T_1 : v_1 &\rightarrow e^{iq_{1x}} v_1, \quad v_2 \rightarrow e^{-i\pi + iq_{1x}} v_2, \quad b_\mu \rightarrow b_\mu, \\ T_2 : v_1 &\rightarrow e^{i\theta} v_2, \quad v_2 \rightarrow ie^{i\theta} v_1, \quad b_\mu \rightarrow b_\mu, \\ P_x : v_1 &\rightarrow e^{-i\gamma} v_1^*, \quad v_2 \rightarrow -e^{-i\gamma} v_2^*, \quad b_x \rightarrow b_x, \quad b_y \rightarrow -b_y, \quad b_t \rightarrow -b_t \\ P_y : v_1 &\rightarrow v_2, \quad v_2 \rightarrow v_1, \quad b_x \rightarrow b_x, \quad b_y \rightarrow -b_y, \quad b_t \rightarrow b_t \\ T : v_a &\rightarrow v_a^*, \quad b_\mu \rightarrow b_\mu. \end{aligned} \quad (3.16)$$

where again  $\gamma$  and  $\theta$  are two incommensurate angles when the lattice is distorted. For an isotropic triangular lattice,  $\theta = -\pi/12$ ,  $\gamma = \pi/6$ , and they will continuously evolve to vison model III by tuning the distortion of the lattice.

Finally, let us move to the case where the four minima in the vison band merge to two. In model I,  $v_1$  and  $v_2$  merge together, while in model II  $v_1$  and  $v_2^*$  merge together. But  $v_1$  and  $v_2^*$  carry opposite gauge charges in the CS theory, and so this merger violates the gauge

invariance. So if we want to evolve smoothly from four minima to two minima, we have to take model I.

After the merger, the two minima are located at  $(\pi/2, \pi/2)$  and  $(-\pi/2, -\pi/2)$ . So we have just to use one component complex vison  $v$ , and its PSG leads to

$$\begin{array}{l}
\text{Visons, Model III} \\
T_1 : v \rightarrow iv, \quad b_\mu \rightarrow b_\mu \\
T_2 : v \rightarrow -e^{3\pi i/4}v^*, \quad b_\mu \rightarrow -b_\mu \\
P_x : v \rightarrow -iv^*, \quad b_x \rightarrow b_x, \quad b_y \rightarrow -b_y, \quad b_t \rightarrow -b_t \\
P_y : v \rightarrow v^*, \quad b_x \rightarrow -b_x, \quad b_y \rightarrow b_y, \quad b_t \rightarrow -b_t \\
T : v \rightarrow v^*, \quad b_\mu \rightarrow -b_\mu
\end{array} \tag{3.17}$$

Finally, we consider the nature of the vison order parameters  $v_a v_b$  and  $v_a^* v_b$  which appear in the phases in Fig. 3.

The simplest case is model III, with only one complex vison  $v$ , in which case the only non-trivial order parameter is  $v^2$ . From the PSG, we see that  $v^2$  is the square lattice VBS order parameter, associated with the VBS state shown in Fig. 2. Using the definitions  $V_{\bar{x}, \bar{y}}$  for this order parameter in Ref. 3, we have  $V_{\bar{x}} \sim \cos(\phi + \pi/4)$ ,  $V_{\bar{y}} \sim \cos(\phi - \pi/4)$  where  $v^2 = \exp(i\phi)$ . Here (and henceforth), the axes  $\bar{x}, \bar{y}$  refer to the principle axes of the “square” lattice formed by the  $J$  bonds in Fig. 1.

The vison order parameters for the other models also describe VBS orders but of a different nature. The vison operator  $v_a$  is subject to a  $Z_2$  gauge invariance, therefore the physical VBS order parameter should always be bilinear of  $v_a$ . There are in total 15 independent bilinear of  $v_a$ , and the detailed VBS pattern drive by vison proliferation depends on the Hamiltonian of visons, which will be discussed in the next section.

#### IV. PHASE DIAGRAMS

Now we turn to the crucial question of combining the spinon and vison PSGs in Section III into consistent theories of the form in Eq. (1.1). We will denote the resulting theories by an obvious notation *i.e.* the theory BIII has spinons under model B and visons under model III.

In principle, there are now 6 possible theories, AI, AII, AIII, BI, BII, and BIII, and associated phase diagrams. To establish the consistency of these theories, we have to examine the transformation of the CS term under the respective spinon and vison PSGs. The results of such an analysis are summarized in Table I for all theories. We see that under theories BI and BIII the Chern Simons term is strictly invariant, and so these theories are clearly consistent. For the remaining theories, the overall form of the CS term remains invariant, but some of the transformations do lead to a change in sign of the CS term. However, the role of the CS term here for  $k = 2$  is only to implement a mutual semionic phase of  $\pi$ ,

	BI and BIII	AI and AIII	AII	BII
$T_1$	+	+	+	+
$T_2$	+	−	+	−
$P_x$	+	−	−	+
$P_y$	+	+	−	−
$T$	+	−	−	+

TABLE I: Transformation of the mutual Chern Simons term under the space group operations for the various theories. The CS term changes its overall sign, as indicated.

and this is invariant under the sign change. Equivalently, we are free to define the vison at momentum  $\mathbf{Q}$  to be either  $v$  or  $v^*$ , which means that in the system there should be particle-hole symmetry of vison *i.e.* on average the spinons see zero flux. This particle-hole symmetry corresponds to the free choice of the sign of gauge charge of vison, and leads to the freedom of the sign of the mutual CS term.

### A. Model AI

The Lagrangian should be invariant under all the symmetry and PSG transformations, which in general takes the form:

$$\begin{aligned}
\mathcal{L} = & \sum_{\alpha=1}^2 \left\{ |(\partial_\mu - ia_\mu)z_\alpha|^2 + s_z |z_\alpha|^2 \right\} + \sum_{a=1}^2 \left\{ |(\partial_\mu - ib_\mu)v_a|^2 + s_v |v_a|^2 \right\} + \frac{ik}{2\pi} \epsilon_{\mu\nu\lambda} a_\mu \partial_\nu b_\lambda \\
& + u_z \left( \sum_{\alpha=1}^2 |z_\alpha| \right)^2 + u_v \left( \sum_{a=1}^2 |v_a| \right)^2 + g |v_1|^2 |v_2|^2 + \dots
\end{aligned} \tag{4.1}$$

Let us first identify all the symmetries of this Lagrangian. The  $U(1)$  gauge symmetries associated with gauge field  $a_\mu$  and  $b_\mu$ , correspond to two global  $U(1)$  symmetries  $U(1)_a \times U(1)_b$  in the dual picture, which lead to the conservation of gauge fluxes. Through the mutual CS term, the gauge flux of  $a_\mu$  is attached with the vison number, and the gauge flux of  $b_\mu$  is attached with the spinon number. On top of the  $U(1)$  gauge symmetries, the global symmetry of this Lagrangian to the fourth order of  $z_\alpha$  and  $v_a$  is  $SU(2)_{\text{spin}} \times U(1) \times Z_2$ . The  $U(1)$  symmetry corresponds to the  $U(1)$  transformation on vison bilinear  $v_1^* v_2$ ; the  $Z_2$  symmetry corresponds to interchanging  $v_1$  and  $v_2$ , which physically can be understood as the reflection symmetry  $P_y$ . If the lattice is an undistorted triangular lattice,  $g = 0$ , and the vison doublet enjoys an enlarged  $SU(2)$  flavor symmetry in this mutual CS theory (or an  $O(4)$  symmetry in a theory with only vison). The ellipses in Eq. (4.1) include terms no

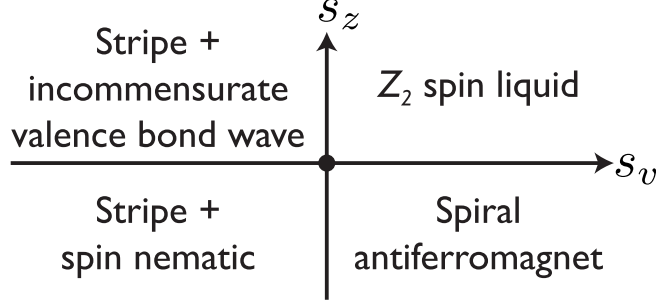


FIG. 5: Phase diagram of model AI with  $g > 0$ . The stripe order is illustrated in Fig. 7, while the spiral antiferromagnet is as in Fig. 2.

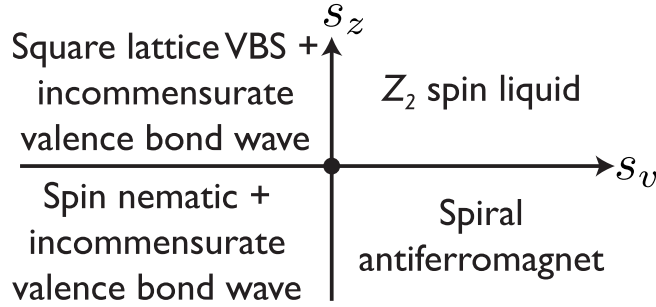


FIG. 6: Phase diagram of model AI with  $g < 0$ . The square lattice VBS state is as illustrated in Fig. 2.

less than sixth order of  $v_a$ , which may introduce higher order anisotropy. In the distorted triangular lattice, the lowest order term which breaks the symmetries in Eq. (4.1) is at the eighth order:

$$\mathcal{L}_8 = g_8(v_1 v_2)^4 + \text{H.c.} \quad (4.2)$$

In the undistorted lattice, the lowest order symmetry breaking term is at the sixth order. If only the terms below fourth order are considered, we can minimize the Lagrangian in Eq. (4.1) with tuning parameter  $s_z$  and  $s_v$ , and obtain the phase diagrams in Fig. 5 and 6, with the phases described in the following subsections.

#### 1. The $Z_2$ spin liquid and spiral phases

The phase with both the spinons and visons gapped out ( $s_z > 0$ ,  $s_v > 0$ ) is the  $Z_2$  spin liquid, as was discussed in Sections I and II, has four-fold topological degeneracy on a compact torus. The phase with visons gapped and spinons condensed ( $s_v > 0$ ,  $s_z < 0$ ), is the incommensurate spin spiral state, with wave vector  $\mathbf{Q}$ . With the vison gapped, the

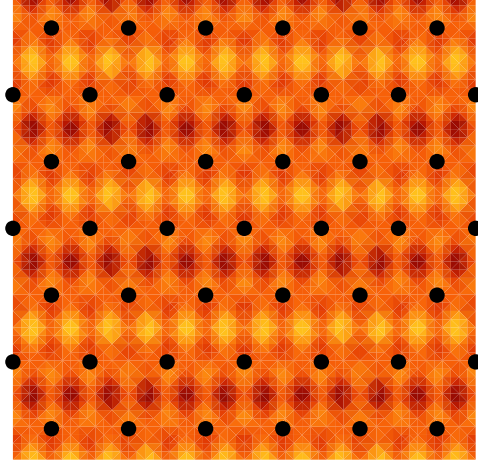


FIG. 7: Illustration of the  $Z_2$  stripe order. This can be viewed as a bond density wave, with alternating signs on successive rows of bonds.

gauge field  $b_\mu$  is in the photon phase, and so the CS term “Higgses” out the gauge field  $a_\mu$ . Or more precisely, for  $k = 2$ , one gauge flux of  $b_\mu$  carries two gauge charges of  $a_\mu$ ; therefore the photon phase of  $b_\mu$ , which is the superfluid phase of gauge flux, breaks the  $U(1)$  gauge invariance of  $a_\mu$  to  $Z_2$ , as was discussed in Section II. As also noted in Section II, this implies that the GSM of the spinon condensate is  $S^3/Z_2$ , and this is the GSM of the spiral spin state. Another way to understand this phase is that, because the vison number is attached with the flux number of  $a_\mu$  through the mutual CS term, in the Mott insulator phase of vison the photon of  $a_\mu$  is gapped out, while  $b_\mu$  is in the photon phase. The global symmetry  $U(1)_b$  becomes the global  $U(1)$  symmetry of the spinon  $z_\alpha$ , which according to the PSG in Eq. (3.5) corresponds to the physical translation transformation.

## 2. The vison condensate with $s_v < 0$ and $s_z > 0$

The nature of the phase with spinon gapped and vison condensed depends on the sign of  $g$  in Eq. (4.1). With the spinon gapped, the  $U(1)$  gauge field  $b_\mu$  is broken down to  $Z_2$  gauge field. Integrating out the remnant  $Z_2$  gauge field, the vison  $v_a$  enjoys a  $U(1) \times U(1) \times Z_2$  symmetry. The two  $U(1)$ s correspond to the global symmetry of two flavors of visons respectively, and the  $Z_2$  symmetry corresponds to the interchange symmetry between  $v_1$  and  $v_2$ . With  $g > 0$ , the vison condensate breaks the  $U(1) \times U(1) \times Z_2$  symmetry to  $U(1)$  symmetry *i.e.* only one flavor of  $v_a$  condenses. Let us assume  $z_1$  condenses, and  $z_2$  remains gapped. The GSM of the vison condensate is  $S^1 \times Z_2$ . The  $Z_2$  degeneracy is described by the Ising order parameter  $v^\dagger \sigma^z v$ , which corresponds to the stripe order depicted in Fig. 7. The  $S^1$  in the GSM is described by the order parameter  $v_1^2$ , which corresponds to an incommensurate valence bond density wave along the  $x$  direction with wave vector  $(2q_{1x}, \pi)$ , meanwhile

breaks the Ising symmetry of interchanging  $v_1$  and  $v_2$ , or the reflection symmetry  $P_y$ . The continuous symmetry  $U(1)$  transformation of  $v_1$  which has been broken by this valence bond density wave is the translation along  $\hat{x}$ . Because  $v_1$  carries an incommensurate momentum, the full Lagrangian in (4.1) with all the higher order perturbation should preserve this global  $U(1)$  symmetry, and the GSM  $S^1 \times Z_2$  is not broken down to smaller manifolds. For instance, the eighth order term  $\mathcal{L}_8$  violates the vison numbers of both  $v_1$  and  $v_2$ , in the phase with only  $v_1$  condensed,  $\mathcal{L}_8$  is suppressed.

If  $g < 0$ , the vison condensate breaks its global symmetry to  $Z_2$  *i.e.* both  $v_1$  and  $v_2$  condense with equal stiffness, the GSM is  $S^1 \times S^1$  if there are no more symmetry breaking terms. The two  $S^1$  corresponds to two  $U(1)$  order parameters  $v_1 v_2$  and  $v_1^* v_2$  respectively. The  $U(1)$  symmetry of  $v_1^* v_2$  is preserved by the full Lagrangian, while the  $U(1)$  symmetry of  $v_1 v_2$  is broken by the eighth order term  $\mathcal{L}_8$  in Eq. (4.2). This term breaks the  $U(1)$  symmetry of  $v_1 v_2$  to  $Z_4$  symmetry. Actually, the order parameter  $v_1 v_2$  corresponds to the  $Z_4$  degeneracy of the four VBS states, which are smoothly connected to the four fold degenerate VBS states in the square lattice limit with  $J' \sim 0$ . Using the square lattice coordinates, the VBS order parameters are

$$\begin{aligned} V_{\bar{x}} &\sim v_1 v_2 \exp(i\pi/4) + v_1^* v_2^* \exp(-i\pi/4), \\ V_{\bar{y}} &\sim v_1 v_2 \exp(-i\pi/4) + v_1^* v_2^* \exp(i\pi/4). \end{aligned} \quad (4.3)$$

The square lattice VBS order is selected when  $g_8 > 0$ , otherwise the four fold degenerate plaquette state is favored. On top of this commensurate VBS order, an incommensurate valence bond density wave corresponding to  $v_1^* v_2$  is also present, with wave vector  $(\pi - 2q_{1x}, 0)$ .

### 3. The phase with both spinons and visons condensed, $s_z < 0$ , $s_v < 0$

The most interesting phase is the phase with both spinons and visons condensed. In this phase, the physical order parameter should be the  $U(1)$  gauge invariant bilinears of  $z_\alpha$  and  $v_a$ , as discussed in Section II. The spin order parameter is the nematic vector  $\vec{n}_3 \sim z^\dagger \sigma^a z$ . The VBS pattern, depending on the sign of  $g$ , is either the  $Z_2$  order parameter  $v^\dagger \sigma^z v$ , or the incommensurate valence bond density wave  $v_1^* v_2$ . Note however, that the commensurate VBS order parameters  $V_{\bar{x}}$  and  $V_{\bar{y}}$  vanish, because they are not gauge invariant. Another way of understanding the vanishing of  $V_{\bar{x}}$  and  $V_{\bar{y}}$  is as follows: when the spinon  $z_\alpha$  is still condensed, the flux of  $a_\mu$  is in the Mott insulator phase; because the flux number of  $a_\mu$  is attached to the vison number through the mutual CS term, any order parameter violating the vison number conservation should not condense.

The GSM of this phase is either  $S_{spin}^2 \times Z_2$  ( $g > 0$ ) or  $S_{spin}^2 \times S^1$  ( $g < 0$ ). And these GSM are not lifted by any higher order term in the Lagrangian Eq. 4.1.

Also note that  $\mathcal{L}_8$  in Eq. (4.2) violates the gauge symmetry of  $b_\mu$ . In the condensate

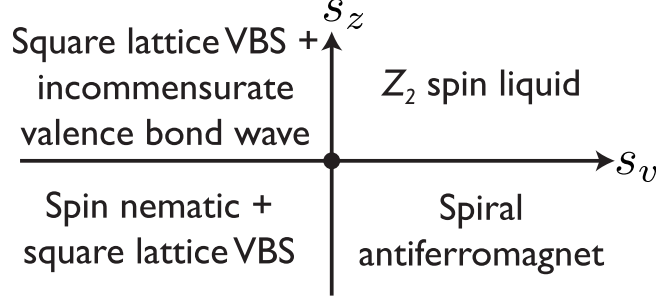


FIG. 8: Phase diagram of model AII with  $g < 0$ . The phase diagram of model AII with  $g > 0$  is the same as that for model AI with  $g > 0$ .

of visons,  $L_8$  confines the fluxes of  $b_\mu$ , and hence the spinon excitation  $z_\alpha$  is also confined, which is consistent with the intuitive understanding of VBS states.

### B. Model AII

The phase diagram of this model is very similar to the previous subsection, the model AI. The only difference is that we now replace  $v_2$  by  $v_2^*$ . So the spiral spin density wave, the  $Z_2$  spin liquid, and the VBS order are the same as in model AI. The commensurate VBS order parameter is now represented as

$$\begin{aligned} V_{\vec{x}} &\sim v_1 v_2^* \exp(i\pi/4) + v_1^* v_2 \exp(-i\pi/4), \\ V_{\vec{y}} &\sim v_1 v_2^* \exp(-i\pi/4) + v_1^* v_2 \exp(i\pi/4). \end{aligned} \quad (4.4)$$

And the incommensurate valence bond wave is represented by  $v_1 v_2$ .

In model AII, the VBS pattern with both spinons and visons condensed is different from model AI. Because in this phase all the physical order parameters should be U(1) gauge invariant, the VBS order parameter is either the  $Z_2$  symmetry breaking  $v^\dagger \sigma^z v$ , or the  $Z_4$  symmetry breaking  $V_{\vec{x}}$  and  $V_{\vec{y}}$  depending on the sign of  $g$ . The GSM is  $S_{spin}^2 \times Z_2$  ( $g > 0$ ) or  $S_{spin}^2 \times Z_4$  ( $g < 0$ ). The phase diagram is shown in Fig. 8.

### C. Model AIII

In this model there is only one complex vison. The  $Z_2$  spin liquid and the spiral spin state are the same as the two previous models. The vison condensate induces the four fold degenerate VBS order, with order parameter  $V_{\vec{x}} \sim v^2 \exp(i\pi/4) + h.c.$ ,  $V_{\vec{y}} \sim v^2 \exp(-i\pi/4) + h.c.$ . However, one can no longer write down a U(1) gauge invariant order parameter in terms of  $v$ , therefore the phase with both spinons and visons condensed has only the nematic order  $\vec{n}_3$ , and no other lattice symmetry breaking. The phase diagram is shown in Fig. 9.

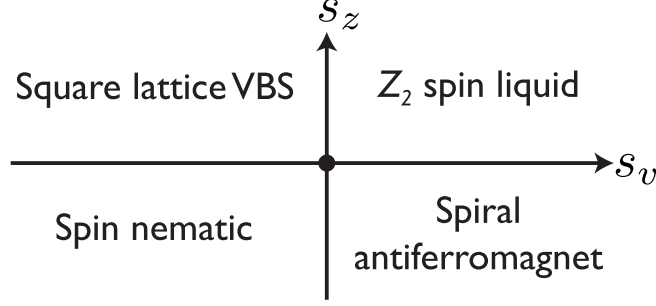


FIG. 9: Phase diagram of model AIII.

If the parameter  $t'/t$  is tuned, the four vison minima will merge to two vison minima *i.e.* the two complex visons become one complex vison. Therefore by tuning  $t'/t$ , model AIII can be connected to model AI.

#### D. Models BI, BII, BIII

These models are similar to models AI, AII, AIII. The main difference is that, in the phase with both spinons and visons condensed, the spin order is the collinear Néel order, in place of the spin nematic order parameter. The phase diagram for model BIII was shown in Fig. 2.

We now discuss in some detail how the spiral order emerges in model B, as this is not evident from the underlying spin representation in Eq. (3.6). If we use only the constraints imposed by the model B PSG in Eq. (3.8), then the Lagrangian of the spinons allows an additional linear spatial derivative term: In the Lagrangian of spinon of

$$\mathcal{L}_x \sim \epsilon_{\alpha\beta} z_\alpha \nabla_x z_\beta + \text{H.c.} \quad (4.5)$$

The term  $\mathcal{L}_x$  violates the enlarged U(1) gauge invariance of the mutual CS Lagrangian discussed below Eq. (3.6). The mutual CS term will bind this term with the monopole operator of  $b_\mu$ , which creates  $2\pi b_\mu$  gauge flux. We denote this monopole operator by  $\mathcal{M}_b$ , then in the U(1) gauge invariant formalism  $\mathcal{L}_x$  reads

$$\mathcal{L}_x \sim \mathcal{M}_b \epsilon_{\alpha\beta} z_\alpha \nabla_x z_\beta + \text{H.c.} \quad (4.6)$$

In the phase with both spinons and visons condensed, the term  $\mathcal{L}_x$  is suppressed, because of the conservation of the flux of  $b_\mu$  which is attached to the spinon number of  $z_\alpha$ . However, once the visons are gapped, the monopoles  $\mathcal{M}_b$  condense and  $\mathcal{L}_x$  becomes relevant. Due to its linear derivative of  $x$ ,  $\mathcal{L}_x$  will drive the system into an incommensurate spiral state with wave vector along  $\hat{x}$  axis, as has been described in Ref. 8. The size of the incommensurate



wave vector increases linearly with  $\langle \mathcal{M}_b \rangle \sim \sqrt{\rho_b}$ , where  $\rho_b$  is the stiffness of the  $b_\mu$  flux condensate, which is proportional to the gap of vison.

## V. QUANTUM PHASE TRANSITIONS

There are many phase transitions involved in the phase diagrams discussed in Section IV. We will study them in the same manner as the previous section.

Before turning to the individual cases, it is useful to discuss an alternative form of the mutual CS theories, Eq. (1.1). For many of the vison models, it is possible to<sup>60,61</sup> “undualize” the vison degrees of freedom: this leads to an alternative formulation of the theory, now without a CS term. This new undualized form will be useful for many purposes.

Let us first consider the simplest case of a single complex vison, as in model III. By the usual boson-vortex duality<sup>60</sup>, the dual of  $v$  is the monopole operator  $\mathcal{M}_b$  introduced below Eq. (4.6). This monopole operator carries charge  $k = 2$  under  $a_\mu$ , and consequently we can write the theory for the two-component spinor  $z_\alpha$  and the complex “Higgs” scalar  $\mathcal{M}_b$ : Thus a theory equivalent to Eq. (1.1) for models AIII and BIII is

$$\begin{aligned} \mathcal{L}_M = & \sum_{\alpha=1}^2 \left\{ |(\partial_\mu - ia_\mu)z_\alpha|^2 + s_z |z_\alpha|^2 \right\} + |(\partial_\mu + 2ia_\mu)\mathcal{M}_b|^2 - s_v |\mathcal{M}_b|^2 \\ & + u_z \left( \sum_{\alpha=1}^2 |z_\alpha|^2 \right)^2 + u_M |\mathcal{M}_b|^4 + v_M |\mathcal{M}_b|^2 \left( \sum_{\alpha=1}^2 |z_\alpha|^2 \right) \\ & + \lambda (\mathcal{M}_b \epsilon_{\alpha\beta} z_\alpha \partial_x z_\beta + \text{H.c.}). \end{aligned} \quad (5.1)$$

The  $\lambda$  term descends from Eq. (4.6), and is present only for model BIII. A closely related model, for a similar model, was obtained directly from the Schwinger boson formulation in Ref. 8. Note that we have (schematically) changed the sign of the “mass” term for  $\mathcal{M}_b$  from that for the vison  $v$ . This reflects the dual relation between the fields, and the fact the  $v$  is condensed when  $\mathcal{M}_b$  is gapped, and vice versa. We note that the mapping between the CS theory in Eq. (1.1) and the non-CS theory in Eq. (5.1) is similar to that described for supersymmetric gauge theories in Ref. 50.

A similar (un)duality mapping can be applied to visons in model I and II. This mapping only works for the  $g < 0$  (“easy-plane”) case of the theory in Eq. (4.1). In this case, the vison fields  $v_{1,2}$  and the gauge field  $b_\mu$  form an easy-plane  $\text{CP}^1$  model, and so we can directly use the duality mappings of Ref. 61. The dual theory is yet another  $\text{CP}^1$  model, with fields  $m_1$  and  $m_2$  and a gauge field  $c_\mu$ . Here  $m_{1,2}$  are merons in the vison  $\text{CP}^1$  model, and the monopole in the  $b_\mu$  field is<sup>3,61</sup>  $\mathcal{M}_b \sim m_1 m_2$ . Thus a new form of the theory (4.1) for models

AI, AII, BI, BII with  $g < 0$  is

$$\begin{aligned}
\mathcal{L}_m = & \sum_{\alpha=1}^2 \left\{ |(\partial_\mu - ia_\mu)z_\alpha|^2 + s_z |z_\alpha|^2 \right\} \\
& + |(\partial_\mu + ia_\mu + ic_\mu)m_1|^2 + |(\partial_\mu + ia_\mu - ic_\mu)m_2|^2 - s_v \left\{ |m_1|^2 + |m_2|^2 \right\} \\
& + u_z \left( \sum_{\alpha=1}^2 |z_\alpha|^2 \right)^2 + u_m \left\{ |m_1|^2 + |m_2|^2 \right\}^2 + g_m |m_1|^2 |m_2|^2 \\
& + v_m \left\{ |m_1|^2 + |m_2|^2 \right\} \left( \sum_{\alpha=1}^2 |z_\alpha|^2 \right) + \lambda (m_1 m_2 \epsilon_{\alpha\beta} z_\alpha \partial_x z_\beta + \text{H.c.}). \tag{5.2}
\end{aligned}$$

Again the  $\lambda$  term is present only for models BI and BII. Also the phase diagrams can be mapped by keeping in mind the dual relation between the visons  $v_{1,2}$  and the merons  $m_{1,2}$ : the visons are condensed when the merons are gapped, and vice versa.

Now we will turn to a description of the transitions for the various models, using the theories in Eq. (1.1), (4.1), (5.1) and (5.2).

## A. Phase transitions in model AI

### 1. Transition between $Z_2$ spin liquid and spiral spin state

This transition is known<sup>53,54,55</sup> to be a 3D O(4) transition, and the mutual CS theory does reproduce this O(4) universality class: in the  $Z_2$  spin liquid, the vison is gapped, therefore the gauge field  $a_\mu$  is “Higgsed” by gauge field  $b_\mu$ , and the U(1) gauge symmetry of  $a_\mu$  is broken down to the  $Z_2$  gauge symmetry. The critical point described by spinon  $z_\alpha$  enjoys an enlarged O(4) symmetry.

### 2. Transition between $Z_2$ spin liquid and the VBS state

The nature of this transition depends on the sign of  $g$ . When  $g < 0$ , the Lagrangian describing this transition is

$$\mathcal{L} = \sum_{a=1}^2 | \partial_\mu v_a |^2 + r |v_a|^2 + u_v |v_a|^4 + (2u_v + g) |v_1|^2 |v_2|^2 + g_8 v_1^4 v_2^4. \tag{5.3}$$

This Lagrangian describes two coupled 3D XY transitions. The coupling  $g_8$  is clearly irrelevant at this 3D XY transition. The scaling dimension of  $u_{12} = 2u_v + g$  is  $2/\nu - D < 0$ , therefore is also irrelevant ( $\nu$  is the critical exponent defined as  $\xi \sim r^{-\nu}$  at the 3D XY transition, which is greater than 2/3). So the transition between the  $Z_2$  spin liquid and the

VBS order is two copies of 3D XY transitions when  $g < 0$ .

When  $g > 0$ , the transition breaks the  $U(1) \times Z_2$  symmetry. There can be one single first order transition or two separate transitions, with 3D XY and 3D Ising universality class respectively. If the triangular lattice is undistorted,  $g = 0$ , there is one single transition between the  $Z_2$  spin liquid and the VBS order, which belongs to 3D O(4) universality class.

### 3. Transition between spiral spin state and the nematic+VBS state

If  $g < 0$  ( $g > 0$ ), this transition is described by a  $CP^1$  Lagrangian with easy plane (easy axis) limit:

$$\mathcal{L} = \sum_{a=1}^2 |(\partial_\mu - ib_\mu)v_a|^2 + s_v|v_a|^2 + \dots \quad (5.4)$$

The eighth order anisotropy term  $\mathcal{L}_8$  is suppressed at this transition, because the condensate of spinon is the Mott insulator phase of the flux of  $a_\mu$ , which guarantees the conservation of total vison number.

### 4. Transition between VBS order and nematic order

This is a  $CP^1$  transition described by spinon  $z_\alpha$  and  $U(1)$  gauge field  $a_\mu$ . The eighth order anisotropy term of vison  $v_1^4 v_2^4 + h.c.$  violates the conservation of the flux of  $a_\mu$  *i.e.* it corresponds to the instantons in the 2+1d space time which creates/annihilates gauge fluxes. Because  $k = 2$  in Eq. (4.1), one flux of  $a_\mu$  carries two visons, therefore  $\mathcal{L}_8$  corresponds to a quadrupole process. If  $g > 0$ , only one component of  $v_1$  and  $v_2$  condenses, the quadrupole process which involves both  $v_1$  and  $v_2$  is suppressed. However, if  $g < 0$ , the quadrupole process is present, but expected to be irrelevant at the  $CP^1$  critical point<sup>3</sup>. We note here recent numerical studies of the  $CP^1$  field theories, which include indications that this transition is weakly first order<sup>61,63,64,65,66,67</sup>.

One other issue to notice is that the spinon velocity and the vison velocity do not have to be equal. Therefore in the  $CP^1$  models described above, the velocity of matter fields and the velocity of gauge fields are essentially different. In the large  $N$  limit, the  $U(1)$  gauge field has scaling dimension 1, and the one-loop self-energy of gauge field leads to the same velocity as the matter fields. The term with velocity anisotropy has scaling dimension 4, and hence is irrelevant for large enough  $N$ .

## B. Phase transitions in model AII

The phase transitions in model AII are similar to model AI. The only difference is that the eighth order vison term  $\mathcal{L}_8 = g_8(v_1 v_2^*)^4 + h.c.$  conserves the total flux number of  $a_\mu$ , therefore there is no quadrupole process at the transition between the nematic order and the VBS order.

## C. Phase transitions in model AIII

In model AIII, the transition between the spiral spin order and the  $Z_2$  spin liquid is still O(4), while the transition between the  $Z_2$  spin liquid and the VBS order is a 3D XY transition (with an irrelevant eighth order anisotropy), because there is only one flavor of vison.

The transition between the spiral spin order and the nematic spin order is an inverted 3D XY transition<sup>60</sup>, or a  $CP^0$  model with one component of complex boson  $v$  coupled with the U(1) gauge field  $b_\mu$ . The transition between the nematic order and the VBS order is a  $CP^1$  transition with irrelevant quadrupoles.

## D. Phase transitions in model BI, BII and BIII

The transitions in the models with spinon B are similar to the models with spinon A. The major concern is the effect of  $\mathcal{L}_x$  in Eq. (4.6) at the critical points. As discussed in Section IV D, this term is only effective when the vison is gapped or critical, for instance the transition between the  $Z_2$  spin liquid and the spiral antiferromagnet. The theory for this transition with spinon A was the O(4) model. With the term  $\mathcal{L}_x$  present in model B, we can redefine the spinon field using a  $x$ -dependent O(4) rotation to absorb the linear  $x$  derivative<sup>8</sup>. The transition is therefore seen to remain in the O(4) class in model B.

At the transition between the Néel order and spiral order, the field theory is given by a  $CP^{(N-1)}$  model with  $N$  flavors of visons ( $N = 1$  or  $2$ ) and gauge field  $b_\mu$ .  $\mathcal{L}_x$  violates the conservation of spinon, and hence corresponds to a monopole term  $\mathcal{M}_b$  of  $b_\mu$ . For simplicity, let us consider the model BIII with one vison component as an example. Here we can analyze the Néel-spiral transition from the theory in Eq. (5.1) by condensing the monopole operator  $\mathcal{M}_b$ . We parametrize the spinon  $z$  as  $z = e^{i\alpha}(e^{i\phi/2} \cos(\theta/2), e^{-i\phi/2} \sin(\theta/2))^t$ , where  $\alpha$  is a gauge dependent phase angle coupled with the gauge field  $a_\mu$ . Then the effective Lagrangian can be written as

$$L = (\partial_\mu \theta)^2 + (\sin \theta)^2 (\partial_\mu \phi)^2 + \tilde{\lambda} (\nabla_x \theta \text{Re}[\tilde{\mathcal{M}}_b] + \nabla_x \phi \sin \theta \text{Im}[\tilde{\mathcal{M}}_b]). \quad (5.5)$$

where  $\tilde{\mathcal{M}}_b$  is the gauge invariant monopole  $\tilde{\mathcal{M}}_b = \mathcal{M}_b e^{2i\alpha}$ . Integrating out the gapless spin-waves  $\phi$  and  $\theta$ , a singular long range dipole interaction is generated for field  $\tilde{\mathcal{M}}_b$  with

momentum dependence  $q_x^2/(q^2 + \omega^2)$ , which will change the relative scaling dimension between  $x$  and  $y$ ,  $\tau$ . The effective theory for XY field  $\Psi \sim \tilde{\mathcal{M}}_b$  can be viewed as an effective  $z = 2$  theory with scaling dimension  $\Delta[q_x] = 2\Delta[q_y] = 2\Delta[\omega] = 2$ :

$$L_\Phi = \frac{q_x^2}{q_y^2 + \omega^2} |\Psi|^2 + (q_y^2 + \omega^2) |\Psi|^2 + g |\Psi|^4 + \dots \quad (5.6)$$

The upper critical dimension of this  $z = 2$  field theory is  $d = 2$ , therefore this transition will be a mean field transition instead of a 3D XY transition.

For  $N_v = 2$  theories in Eq. 5.2, a similar dipolar term is generated at the quartic term for  $m_i$ , a more detailed analysis is required to determine the fate of this quartic term.

### E. Isotropic triangular lattice

This subsection will briefly comment on the modifications of our results for the case of the isotropic triangular lattice, with  $J' = J$  and full six-fold rotation symmetry.

There is one more symmetry that needs to be considered: the  $2\pi/3$  rotation. Under this rotation, the visons of model II transform as

$$R_{2\pi/3} : v_1 \rightarrow \frac{1}{\sqrt{2}} e^{-i\pi/4} v_1 + \frac{1}{\sqrt{2}} v_2, \quad v_2 \rightarrow -\frac{1}{\sqrt{2}} v_1 + \frac{1}{2} e^{\pi i/4} v_2. \quad (5.7)$$

This PSG transformation is consistent with the enlarged U(1) gauge symmetry; while in model I, visons will be mixed with its complex conjugates, therefore on the isotropic triangular lattice only model II of visons is consistent. Further, the spinon minima are located at the commensurate wave vectors  $\vec{Q} = (2\pi/3, 0)$  and  $-\vec{Q} = -(2\pi/3, 0)$ , and therefore under translation spinons in model A will merely gain a phase factor, while in model B spinons will be mixed with their complex conjugates. Therefore on the isotropic triangular lattice, only model AII is consistent with the enlarged U(1) gauge symmetries.

In the mutual CS theory of model AII on the isotropic lattice,  $g = 0$ , in the phase with both spinon and vison condensed, the VBS order parameter is described by the SU(2) vector  $v^\dagger \sigma^a v$ , which corresponds to degenerate stripe orders  $V_{\bar{x}}$ ,  $V_{\bar{y}}$  in Eq. (4.4), and  $V_z = v^\dagger \sigma^z v$  depicted in Fig. 7, these stripe orders are connected to each other through rotation  $R_{2\pi/3}$ . Notice that, on the distorted triangular lattice, stripe order  $V_{\bar{x}}$  has the same symmetry as the square lattice VBS order.

Because  $g = 0$ , the global symmetry of vison up to the forth order term is SU(2) in the mutual CS theory, and O(4) in the theory with only visons. The GSM of the phase with both spinon and vison condensed is  $S^2 \times S^2$  as far as the forth order terms are considered. Therefore the transition between the  $Z_2$  spin liquid and the VBS order is a 3D O(4) transition<sup>16</sup>, and the transition between the nematic/VBS order to the spiral order in phase diagram Fig. 8 is a  $CP^1$  transition. The PSG of visons allow a sixth order anisotropy term

on the isotropic triangular lattice<sup>16</sup>:

$$L_6 = g_6(v_1 v_2^5 + v_2 v_1^5 + H.c.) \quad (5.8)$$

This term corresponds to the triple monopole process in the dual picture, which annihilates/creates three fluxes of gauge field  $a_\mu$ . This triple monopole is expected to be relevant when gauge field  $a_\mu$  is gapless, which will likely drive the transition between the nematic/VBS and the VBS phase to a first order transition.

### F. Multicritical point, $s_z = s_v = 0$

We now study the multicritical point with both spinons and visons gapless: this is the point M in Fig. 3.

The most convenient way of studying M is likely via the non-CS theories in Eqs. (5.1) and (5.2), although these do not apply for the  $g > 0$  cases. This formulation should be amenable to direct numerical study.

For analytic results, the only available tool is the  $1/N$  expansion, for this we may as well work with the original CS theory in Eq. (1.1). This expansion relies on the assumption that in Eq. (4.1)  $N \sim N_v \sim k$  is large. The  $\lambda$  term in Eq. 5.1 and 5.2 generalizes to terms with  $k$  powers of  $z_\alpha$ , and these are surely irrelevant for large  $k$ . So we ignore the influence of  $\mathcal{L}_x$  for models B in the  $1/N$  expansion.

A systematic  $1/N$  expansion for the  $\text{CP}^{(N-1)}$  model has been calculated previously<sup>68,69</sup>: the  $1/N$  correction comes from the one-loop propagator of both the Lagrange multiplier  $\lambda$  and gauge field  $a_\mu$ :

$$\mathcal{L} = \frac{1}{g} |(\partial_\mu - i a_\mu) z|^2 + i \lambda (|z|^2 - 1) + \dots \quad (5.9)$$

The one loop propagator of  $\lambda$  and  $a_\mu$  are:

$$\begin{aligned} D_{\mu\nu} &= \frac{1}{\Pi_A} \left( \delta_{\mu\nu} - \zeta \frac{q_\mu q_\nu}{q^2} \right), \quad \Pi_A = \frac{Np}{16}, \\ D_\lambda &= \frac{1}{\Pi_\lambda}, \quad \Pi_\lambda = \frac{Np}{8}. \end{aligned} \quad (5.10)$$

For instance, we can calculate the anomalous dimension  $\eta_N$  of gauge invariant operator  $z^\dagger T^a z$  defined as  $\Delta[z^\dagger T^a z] = (D - 2 + \eta_N)/2$ , and  $T^a$  is one of the generators of  $\text{SU}(N)$  algebra; note that this operator is the magnetic order parameter for model B, and the spin nematic order parameter for model A. In the  $\text{CP}^{(N-1)}$  model, the anomalous dimension  $\eta_N$

was calculated in detail in Reference 69, and the result is

$$\eta_N = 1 + \frac{32}{3\pi^2 N} - \frac{128}{3\pi^2 N}. \quad (5.11)$$

The second term on the r.h.s. of the equation above comes from the Lagrange multiplier, while the third term comes from the gauge field.

After including the vison multiplet  $v_a$  and mutual CS term, the  $\lambda$  propagator is unaffected, while the gauge field propagator is modified:

$$D_{\mu\nu} = \frac{1}{\tilde{\Pi}_A} \left( \delta_{\mu\nu} - \zeta \frac{q_\mu q_\nu}{q^2} \right), \quad \tilde{\Pi}_A = \frac{Np}{16} \left( 1 + \frac{64k^2}{\pi^2 N^2} \right). \quad (5.12)$$

All the calculations can be carried out straightforwardly by replacing  $\Pi_A$  in Ref. 69 by  $\tilde{\Pi}_A$ . When  $k \sim N$ , the correction from the vison and mutual CS theory to the anomalous dimension  $\eta_N$  is at the order of  $1/N$ :

$$\eta_N = 1 + \frac{32}{3\pi^2 N} - \frac{128}{3\pi^2 N} \times \frac{1}{1 + 64k^2/(\pi^2 N^2)}. \quad (5.13)$$

All the other critical exponents can be calculated in a similar way.

## VI. BEYOND U(1) CHERN-SIMONS THEORIES

In the previous sections, the global phase diagrams and nature of phase transitions were studied with the mutual CS theory. In this section we will try to look at these phases and transitions in a more intuitive and pictorial way. Let us start with the case with undistorted triangular lattice, which has a ground state with spiral antiferromagnetic order. This spiral order is described in terms of the  $z$  by Eq. (3.3).

Intuitively, to destroy magnetic order, the most straightforward way is to proliferate the topological defects in this magnetic order. The fundamental group of the GSM of spiral order is  $\pi_1[\text{SO}(3)] = Z_2$ , which supports a topologically stable half vortex if rewritten in terms of  $z$ . These half vortices become full vortices of vectors  $\vec{n}_i$ ,  $i = 1, 2, 3$  in Eq. (3.3). These vortices can be most easily understood as an ordinary vortices of two of the three vectors  $\vec{n}_i$ , while keeping the third vector uniform in the whole 2d plane: see Fig. 10. The GSM of this state has isometry group  $\text{SO}(4)$ . If the system has the enlarged  $\text{O}(4)$  symmetry at the microscopic level, all the vortices with different uniform vector (UV) will have the same energy. However, the underlying symmetry is only  $\text{SU}(2) \times \text{PSG}$ , so the energy of the vortices depends on the UV. The lattice symmetry guarantees that the vortices with different UVs have the same energy as long as the UVs can be transformed to each other

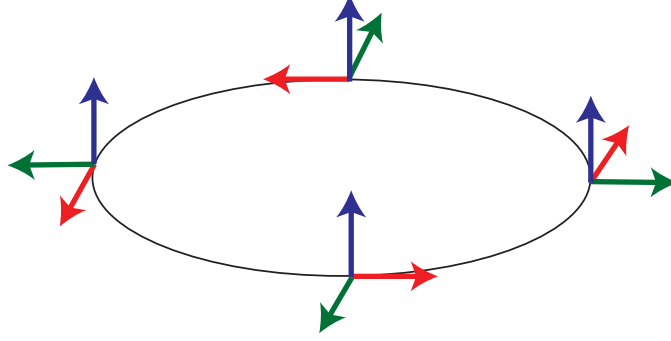


FIG. 10: Schematic of the orientation of the orthogonal vectors  $\vec{n}_1$ ,  $\vec{n}_2$  and  $\vec{n}_3$  around a vortex in the SO(3) GSM of the spiral antiferromagnet. One of the vectors has a constant orientation, while the other two precess by an angle of  $2\pi$ .

through lattice symmetry transformations. There are in total three groups of vortices:

$$\begin{aligned}
 1, \text{ UV} : & \quad \vec{n}_3, \\
 2, \text{ UV} : & \quad \vec{n}_1, \quad -\frac{1}{2}\vec{n}_1 \pm \frac{\sqrt{3}}{2}\vec{n}_2, \\
 3, \text{ UV} : & \quad \vec{n}_2, \quad \pm\frac{\sqrt{3}}{2}\vec{n}_1 - \frac{1}{2}\vec{n}_2.
 \end{aligned} \tag{6.1}$$

All the flavors of vortices in each group have the same energy, while there is no symmetry to protect the degeneracy between different groups. For instance, UV  $\vec{n}_3$  can never be transformed into  $\vec{n}_1$  because of their opposite behavior under time reversal transformation. The first group of vortex has only one flavor, and if we only proliferate this vortex flavor, the spin orders of  $\vec{n}_1$  and  $\vec{n}_2$  are destroyed, while the nematic order  $\vec{n}_3$  is preserved. This leads to a state with GSM  $S^2$ , and it is the situation described by the mutual CS theory AI, AII and AIII. The second and third groups have more than one flavor of vortices, with different flavors of vortices connected to each other through lattice symmetry transformations. If all the flavors of vortices in group 2 or 3 condense, the magnetic order is completely destroyed, and we expect these vortices to drive a direct transition from the  $\sqrt{3} \times \sqrt{3}$  antiferromagnetic spiral order to VBS order. The nature of this transition requires further study, and it cannot be naturally described by our mutual CS theory. In our theory, there are always two tuning parameters ( $s_z$  and  $s_v$ ), and it would require some fine-tuning to induce a direct transition. A theory based on a mutual  $Z_2$  CS formalism has been proposed by another group<sup>70</sup> to describe this direct transition.

One can also condense one flavor of the second or the third group of vortices, which can be realized in the situation with strong repulsions between different flavors of vortices in one group. If the vortex with UV  $\vec{n}_1$  is condensed, the vectors  $\vec{n}_2$  and  $\vec{n}_3$  are disordered, and the



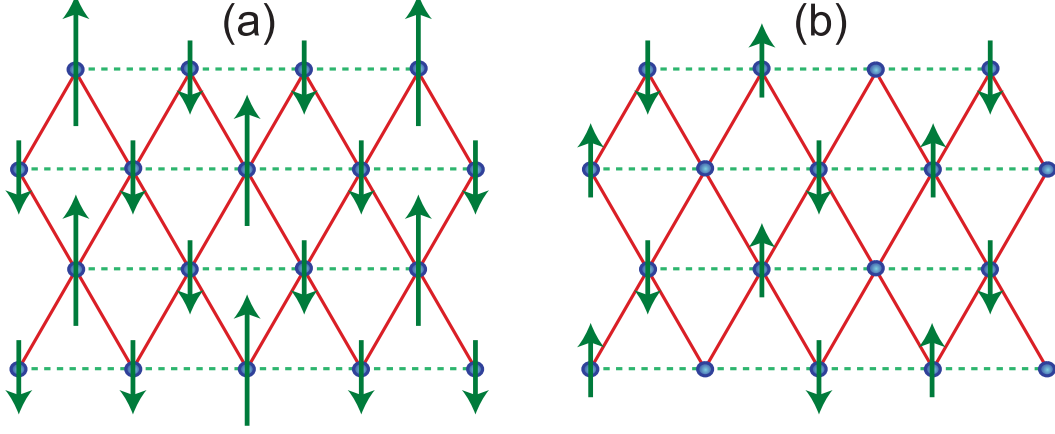


FIG. 11: The remnant spin order pattern after proliferation of one single flavor of group 2 and 3 vortices in Eq. (6.1). (a) Proliferation of the first flavor in group 2, the spin pattern is up-down-down, and the GSM is  $S^2 \times Z_3$ . Notice that the moment of the up spin site is twice as much as the down spin site, so the total magnetization is zero. (b) Proliferation of first flavor in group 3, the spin pattern is up-down-zero with GSM  $S^2 \times Z_3$ .

remnant magnetic order is the up-down-down state in Fig. 11a with zero total magnetization, and the GSM of this up-down-down state is  $S^2 \times Z_3$ . The  $S^2$  corresponds to the direction of  $\vec{n}_1$ , and the  $Z_3$  corresponds to the choice of condensing the three flavors of vortices in the second group of Eq. (6.1), which are connected to each other via translation along the  $x$  axis. If vortex with UV  $\vec{n}_2$  is condensed, the spin pattern becomes the up-down-zero state in Fig. 11b, also with GSM  $S^2 \times Z_3$ . The transition driven by the condensation of vortices with UV  $\vec{n}_1$  and  $\vec{n}_2$  can no longer be described by the U(1) mutual CS theory, because in the phase with both spinons and visons condensed, the physical order parameter of the remnant spin order should be U(1) gauge invariant: thus now one needs a spinon  $z_\alpha$  such that the UV  $n_1 = z^\dagger \sigma^a z$ . However, under translation so-defined spinon  $z_\alpha$  becomes a linear combination between  $z_\alpha$  and  $\epsilon_{\alpha\beta} z_\beta^*$ , which violates the U(1) gauge symmetry.

To consistently describe the transition driven by proliferation of vortices with UV  $\vec{n}_1$  and  $\vec{n}_2$ , a theory based on mutual  $Z_2$  CS theory may be applicable, similar to the  $Z_2$  CS formalism proposed for cuprates<sup>36</sup> where the spinons and half-vortices of the superconducting phase are coupled together through mutual  $Z_2$  CS fields. On the distorted triangular lattice antiferromagnets examined in this work, the mutual  $Z_2$  gauge field also imposes the correct semionic statistics between the spinon and vison. However the  $Z_2$  gauge field can only be conveniently formulated on the lattice, therefore we are unable to comment on all the universal properties of the transitions described by the mutual  $Z_2$  CS theory.

If the triangular lattice is distorted, the spin spiral state becomes incommensurate, and the vector  $\vec{n}_1$  and  $\vec{n}_2$  can be transformed to each other via lattice translation. Therefore

there are only two groups of vortices:

$$\begin{aligned}
1, \text{ UV} : & \quad \vec{n}_3, \\
2, \text{ UV} : & \quad \vec{n}_1, \text{ rotation of } \vec{n}_1 \text{ around } \vec{n}_3.
\end{aligned}
\tag{6.2}$$

The second group of vortices have an infinite number of flavors, and if one of these flavors proliferates, then the spin state becomes a collinear incommensurate spin density wave, which has GSM  $S^2 \times S^1$ . The  $S^2$  corresponds to the remnant spin collinear order, while the  $S^1$  corresponds to translation along  $\hat{x}$  of the incommensurate wave vector.

## VII. CONCLUSIONS AND EXPERIMENTAL IMPLICATIONS

This paper has described examples of a general approach to describing the phases and quantum phase transitions of  $S = 1/2$  antiferromagnets in two dimensions. Our examples were limited to models on the lattice of Fig. 1, because of its experimental importance. However, we expect that similar analysis should be useful *e.g.* on the kagome lattice. Our main results are summarized in phase diagrams, like that in Fig. 2. The same phase diagram was obtained earlier<sup>8</sup> in a more direct microscopic mean field theory, but the nature of the phase transitions and possible multicritical point was left open. Our present, ‘dual’ approach also immediately yields the required critical field theories.

One of the transitions in our phase diagram in Fig. 2 is the Néel-VBS transition, which is described by a  $CP^1$  field theory. This transition has been the focus of much recent numerical work<sup>61,63,64,65,66,67</sup>. The numeric results on the  $S = 1/2$  quantum antiferromagnet strongly support its effective description in terms of the  $CP^1$  field theory. However, some results<sup>65,66</sup> on system sizes larger than  $50 \times 50$  indicate that the transition in the  $CP^1$  model may well be weakly first-order. The multicritical point M has additional flavors of matter fields, and these make it less likely that M is first order. Consequently it would be useful to study M numerically using the theories in Eqs. (5.1) and (5.2): this will help in describing M and the phase diagram in its immediate vicinity. This study can be done with or without the  $\lambda$  coupling in Eqs. (5.1) and (5.2).

As mentioned in Section I, a series of measurements on the distorted triangular lattice materials,  $X[Pd(dmit)_2]_2$ , with different anisotropic coupling  $J'/J$  reveal a possible direct transition between the Néel order and the VBS state, and one particular material with  $X = EtMe_3Sb$  was suggested to be close to the quantum critical point. In our mutual CS theory, as well as the previously proposed deconfined critical point<sup>3</sup>, this transition is described by the  $CP^1$  model with irrelevant quadrupole operators. The quantum critical behaviors at finite temperature can be measured in material  $EtMe_3Sb[Pd(dmit)_2]_2$ . For instance, the NMR relaxation rate  $1/T_1$  scales as  $1/T_1 \sim T^{\eta_N}$ , where  $\eta_N$  is the anomalous dimension of the Néel order parameter at the  $CP^1$  fixed point. Even if the transition in the  $CP^1$  model is

ultimately weakly first order, the critical regime could be observable at intermediate  $T$ , and compared to numerical estimates<sup>63,64,67</sup> of  $\eta_N$ .

We conclude by commenting on the recent interpretation by Ref. 32 of experimental observations on the spin liquid compound  $\kappa$ -(ET)<sub>2</sub>Cu<sub>2</sub>(CN)<sub>3</sub>. Ref. 32 suggested that the very low  $T$  nuclear magnetic resonance was controlled by the O(4) criticality between the spiral and  $Z_2$  spin liquid states, while the intermediate temperature nuclear magnetic resonance (NMR) could be modeled by a multicritical point where both the spinons and visons are gapless. Crucial to this interpretation was the requirement that the anomalous dimension of the magnetic order parameter,  $\eta_N$ , was smaller at the latter multicritical point than at the low  $T$  O(4) critical point.

Here, we have provided examples of such multicritical points, such as the point M in Fig. 2. For spinons in model B, the magnetic order parameter is  $z^\dagger T^a z$ , and its anomalous dimension was computed in Section V F, where we found the result in Eq. (5.13). An important feature of this result is that the U(1) gauge fluctuations reduce the value of  $\eta_N$  from that obtained in the theory without the U(1) gauge field; the latter describes the O(4) transition between the spiral antiferromagnet and the  $Z_2$  spin liquid. Thus model B spinons do fulfill the requirements for the experimental interpretation stated in Ref. 32.

On the other hand, in spinon model A, the order parameter  $z^\dagger T^a z$  represents the nematic order parameter, while the other gauge invariant spinon-monopole composite  $z^t \sigma^y \sigma^a z \mathcal{M}_b$  represents the spiral order parameter. In the case with large  $N_v$ , the scaling dimension of  $\mathcal{M}_b$  is expected to scale linearly with  $N_v$ , and hence to systematically calculate the scaling dimension of  $z^t \sigma^y \sigma^a z \mathcal{M}_b$ , we need an analytical technique beyond the  $1/N$  expansion.

In conclusion, we have proposed a unified theory in the mutual CS formalism to describe all the magnetic phases observed in a series of organic compounds, and discussed the phase transitions between these phases. Experimental implications for organic compounds in the X[Pd(dmit)<sub>2</sub>]<sub>2</sub> series and the  $\kappa$ -(ET)<sub>2</sub>Z series were also discussed.

## Acknowledgments

We thank L. Balents, M. P. A. Fisher, R. Kato, I. Klebanov, P. A. Lee, Y. Qi, T. Senthil, Y. Shimizu, M. Yamashita, and X. Yin for useful discussions. This research was supported by the NSF under grant DMR-0757145, by the FQXi foundation.

---

<sup>1</sup> N. Read and S. Sachdev, Phys. Rev. Lett. **62**, 1694 (1989).

<sup>2</sup> N. Read and S. Sachdev, Phys. Rev. B **42**, 4568 (1990).

<sup>3</sup> T. Senthil, A. Vishwanath, L. Balents, S. Sachdev, and M. P. A. Fisher, Science **303**, 1490 (2004); T. Senthil, L. Balents, S. Sachdev, A. Vishwanath, and M. P. A. Fisher, Phys. Rev. B

- 70**, 144407 (2004).
- <sup>4</sup> O. A. Starykh and L. Balents, Phys. Rev. Lett. **98**, 077205 (2007).
  - <sup>5</sup> M. Kohno, O. A. Starykh, and L. Balents, Nature Physics **3**, 790 (2007).
  - <sup>6</sup> N. Read and S. Sachdev, Phys. Rev. Lett. **66**, 1773 (1991).
  - <sup>7</sup> R. Jalabert and S. Sachdev, Phys. Rev. B **44**, 686 (1991); S. Sachdev and M. Vojta, J. Phys. Soc. Japan **69**, Suppl. B, 1 (2000).
  - <sup>8</sup> S. Sachdev and N. Read, Int. J. Mod. Phys. B **5**, 219 (1991) [arXiv:cond-mat/0402109].
  - <sup>9</sup> S. Sachdev, Phys. Rev. B **45**, 12377 (1992).
  - <sup>10</sup> Z. Weihong, R. H. McKenzie, and R. R. P. Singh, Phys. Rev. B **59**, 14367 (1999).
  - <sup>11</sup> G. Misguich, C. Lhuillier, B. Bernu, and C. Waldtmann, Phys. Rev. B **60**, 1064 (1999).
  - <sup>12</sup> W. LiMing, G. Misguich, P. Sindzingre, and C. Lhuillier, Phys. Rev. B **62**, 6372,6376 (2000).
  - <sup>13</sup> O. I. Motrunich, Phys. Rev. B **72**, 045105 (2005).
  - <sup>14</sup> D. N. Sheng, O. I. Motrunich, S. Trebst, E. Gull, and M. P. A. Fisher, Phys. Rev. B **78**, 054520 (2008).
  - <sup>15</sup> D. Rokhsar and S. A. Kivelson, Phys. Rev. Lett. **61**, 2376 (1988).
  - <sup>16</sup> R. Moessner and S. L. Sondhi, Phys. Rev. B **63**, 224401 (2001).
  - <sup>17</sup> T. Nakamura, T. Takahashi, S. Aonuma, and R. Kato, J. Mater. Chem. **11**, 2159 (2001).
  - <sup>18</sup> M. Tamura and R. Kato, J. Phys.: Condens. Matter **14**, L729 (2002).
  - <sup>19</sup> S. Ohira, M. Tamura, R. Kato, I. Watanabe, and M. Iwasaki, Phys. Rev. B **70**, 220404(R) (2004).
  - <sup>20</sup> M. Tamura, A. Nakao and R. Kato, J. Phys. Soc. Japan **75**, 093701 (2006).
  - <sup>21</sup> Y. Shimizu, H. Akimoto, H. Tsujii, A. Tajima, and R. Kato, Phys. Rev. Lett. **99**, 256403 (2007).
  - <sup>22</sup> Y. Shimizu, H. Akimoto, H. Tsujii, A. Tajima, and R. Kato, J. Phys.: Condens. Matter **19**, 145240 (2007).
  - <sup>23</sup> T. Itou, A. Oyamada, S. Maegawa, M. Tamura, and R. Cato, Phys. Rev. B **77**, 104413 (2008).
  - <sup>24</sup> B. J. Powell and R. H. McKenzie, J. Phys.: Condens. Matter **18**, R827 (2006).
  - <sup>25</sup> K. Miyagawa, A. Kawamoto, Y. Nakazawa, and K. Kanoda, Phys. Rev. Lett. **75**, 1174 (1995).
  - <sup>26</sup> Y. Shimizu, K. Miyagawa, K. Kanoda, M. Maesato, and G. Saito, Phys. Rev. Lett. **91**, 107001 (2003).
  - <sup>27</sup> Y. Shimizu, K. Miyagawa, K. Kanoda, M. Maesato, and G. Saito, Phys. Rev. B **73**, 140407(R) (2006).
  - <sup>28</sup> S. Yamashita, Y. Nakazawa, M. Oguni, Y. Oshima, H. Nojiri, Y. Shimizu, K. Miyagawa, and K. Kanoda, Nature Physics **4**, 459 (2008).
  - <sup>29</sup> M. Yamashita, H. Nakata, Y. Kasahara, S. Fujimoto, T. Shibauchi, Y. Matsuda, T. Sasaki, N. Yoneyama, and N. Kobayashi, unpublished and 25th International Conference on Low Temperature Physics, SaM3-2, Amsterdam, August 9, 2008.
  - <sup>30</sup> S.-S. Lee, P. A. Lee, and T. Senthil, Phys. Rev. Lett. **98**, 067006 (2007).
  - <sup>31</sup> Y. Qi and S. Sachdev, Phys. Rev. B **77**, 165112 (2008).

- <sup>32</sup> Y. Qi, C. Xu, and S. Sachdev, arXiv:0809.0694.
- <sup>33</sup> J. O. Fjærestad, W. Zheng, R. R. P. Singh, R. H. McKenzie, and R. Coldea, Phys. Rev. B **75**, 174447 (2007).
- <sup>34</sup> R. Coldea, D. A. Tennant, A. M. Tsvelik, and Z. Tylczynski Phys. Rev. Lett. **86**, 1335 (2001).
- <sup>35</sup> X. G. Wen, Phys. Rev. B **44**, 2664 (1991).
- <sup>36</sup> T. Senthil and M. P. A. Fisher Phys. Rev. B **62**, 7850 (2000).
- <sup>37</sup> A. Y. Kitaev, Annals of Physics **303**, 2 (2003).
- <sup>38</sup> X. G. Wen, Phys. Rev. Lett. **90**, 016803 (2003).
- <sup>39</sup> M. Freedman, C. Nayak, K. Shtengel, K. Walker, and Z. Wang, Annals of Physics **310**, 428 (2004).
- <sup>40</sup> F. Wang and A. Vishwanath, Phys. Rev. B **74**, 174423 (2006).
- <sup>41</sup> G. Misguich and F. Mila, Phys. Rev. B **77**, 134421 (2008).
- <sup>42</sup> N. Read and B. Chakraborty, Phys. Rev. B **40**, 7133 (1989).
- <sup>43</sup> S.-P. Kou, M. Levin, and X.-G. Wen, arXiv:0803.2300.
- <sup>44</sup> Su-Peng Kou, Xiao-Liang Qi, Zheng-Yu Weng, Phys. Rev. B **71** 235102 (2005).
- <sup>45</sup> J. Bagger and N. Lambert, Phys. Rev. D **75**, 045020 (2007) [arXiv:hep-th/0611108]; Phys. Rev. D **77**, 065008 (2008) [arXiv:0711.0955]
- <sup>46</sup> A. Gustavsson, arXiv:0709.1260.
- <sup>47</sup> M. Van Raamsdonk, JHEP **0805**, 105 (2008) [arXiv:0803.3803].
- <sup>48</sup> O. Aharony, O. Bergman, D. L. Jafferis and J. Maldacena, JHEP **0810**, 091 (2008) [arXiv:0806.1218].
- <sup>49</sup> M. Benna, I. Klebanov, T. Klose and M. Smedback, JHEP **0809**, 072 (2008) [arXiv:0806.1519].
- <sup>50</sup> D. L. Jafferis and X. Yin, arXiv:0810.1243.
- <sup>51</sup> S. Sachdev and X. Yin, arXiv:0808.0191.
- <sup>52</sup> L. Balents and M. P. A. Fisher, Phys. Rev. B **71**, 085119 (2005).
- <sup>53</sup> P. Azaria, B. Delamotte, and T. Jolicoeur, Phys. Rev. Lett. **64**, 3175 (1990).
- <sup>54</sup> A. V. Chubukov, T. Senthil and S. Sachdev, Phys. Rev. Lett. **72**, 2089 (1994).
- <sup>55</sup> S. V. Isakov, T. Senthil, and Y. B. Kim, Phys. Rev. B **72**, 174417 (2005).
- <sup>56</sup> P. W. Anderson, Phys. Rev. **86**, 694 (1952).
- <sup>57</sup> S. Sachdev, Rev. Mod. Phys. **75**, 913 (2003).
- <sup>58</sup> C. Lannert, M. P. A. Fisher, and T. Senthil, Phys. Rev. B **63**, 134510 (2001).
- <sup>59</sup> L. Balents, L. Bartosch, A. Burkov, S. Sachdev, and K. Sengupta, Phys. Rev. B **71**, 144508 (2005).
- <sup>60</sup> C. Dasgupta and B. I. Halperin, Phys. Rev. Lett. **47**, 1556 (1981).
- <sup>61</sup> O. I. Motrunich and A. Vishwanath, Phys. Rev. B **70**, 075104 (2004).
- <sup>62</sup> A. Aharony, Phys. Rev. B **8**, 3363 (1973).
- <sup>63</sup> A. W. Sandvik, Phys. Rev. Lett. **98**, 227202 (2007).
- <sup>64</sup> R. G. Melko and R. K. Kaul, Phys. Rev. Lett. **100**, 017203 (2008); Phys. Rev. B **78**, 014417

- (2008).
- <sup>65</sup> F.-J. Jiang, M. Nyfeler, S. Chandrasekharan, and U.-J. Wiese, arXiv:0710.3926.
- <sup>66</sup> A. B. Kuklov, M. Matsumoto, N. V. Prokof'ev, B. V. Svistunov, and M. Troyer, Phys. Rev. Lett. **101**, 050405 (2008).
- <sup>67</sup> O. I. Motrunich and A. Vishwanath, arXiv:0805.1494.
- <sup>68</sup> V. Yu. Irkhin, A. A. Katanin, and M. I. Katsnelson, Phys. Rev. B **54**, 11953 (1996).
- <sup>69</sup> R. K. Kaul, and S. Sachdev Phys. Rev. B **77**, 155105 (2008).
- <sup>70</sup> S. Bhattacharjee and T. Senthil, unpublished.